

Review

Semiconductor Nanomaterials-Based Fluorescence Spectroscopic and Matrix-Assisted Laser Desorption/Ionization (MALDI) Mass Spectrometric Approaches to Proteome Analysis

Suresh Kumar Kailasa ^{1,†}, Kuang-Hung Cheng ^{2,†} and Hui-Fen Wu ^{3,4,5,6,*}

¹ Department of Chemistry, S. V. National Institute of Technology, Surat 395007, India;
E-Mail: sureshkumarchem@gmail.com

² Institute of Biomedical Sciences, National Sun Yat-Sen University, Kaohsiung 804, Taiwan;
E-Mail: khcheng@faculty.nsysu.edu.tw

³ Department of Chemistry, National Sun Yat-Sen University, Kaohsiung 804, Taiwan

⁴ Center for Nanoscience and Nanotechnology, National Sun Yat-Sen University,
Kaohsiung 804, Taiwan

⁵ Doctoral Degree Program in Marine Biotechnology, National Sun Yat-Sen University,
Kaohsiung 804, Taiwan

⁶ School of Pharmacy, College of Pharmacy, Kaohsiung Medical University, Kaohsiung 806, Taiwan

† These authors contributed equally to this work.

* Author to whom correspondence should be addressed; E-Mail: hwu@faculty.nsysu.edu.tw;
Tel.: +886-7-525-2000 (ext. 3955); Fax: +886-7-525-3908.

Received: 24 July 2013; in revised form: 14 October 2013 / Accepted: 18 October 2013 /

Published: 9 December 2013

Abstract: Semiconductor quantum dots (QDs) or nanoparticles (NPs) exhibit very unusual physico-chemical and optical properties. This review article introduces the applications of semiconductor nanomaterials (NMs) in fluorescence spectroscopy and matrix-assisted laser desorption/ionization mass spectrometry (MALDI-MS) for biomolecule analysis. Due to their unique physico-chemical and optical properties, semiconductor NMs have created many new platforms for investigating biomolecular structures and information in modern biology. These semiconductor NMs served as effective fluorescent probes for sensing proteins and cells and acted as affinity or concentrating probes for enriching peptides, proteins and bacteria proteins prior to MALDI-MS analysis.

Keywords: quantum dots; fluorescent and affinity probes; biomolecules; fluorescence spectroscopy; MALDI-MS

1. Introduction

Nanomaterials have been integrated in various analytical tools to gain prominence advances in bioanalytical and proteomics research communities since last decade. Among many different nanomaterials, the colloidal semiconductor nanocrystals (NCs) or QDs have been demonstrated as potential optical probes in bioanalytical chemistry due to their special physico-chemical and optical properties including size-tunable emission, continuous absorption profile to blue of the band edge and stability against photobleaching which allows a novel and often counter-intuitive applications in bioanalytical research [1–5]. Although several materials exhibit semiconducting behavior, silicon has been most widely used than any other semiconductors. Silicon is a group IV and its outer orbital of an individual atom is only half filled. After in-depth studies on the structural properties of nanomaterials, the colloidal nanocrystalline semiconductors are collectively referred as the comprising elements from the periodic groups II–VI, III–V or IV–VI, are roughly spherical and with sizes typically in the range 1–20 nm in diameter. Over the last two decades, the development of semiconductor nanomaterials has received tremendous progress in their preparation as well as in understanding their optical and electronic properties [6–8]. Indeed, the QDs exhibited tremendous applications in biodiagnostics, bioimaging, photonics, optoelectronics, and sensors [9]. Importantly, different sizes of QDs can be excited simultaneously by a single wavelength and emit with distinctly different colors. In this connection, the swift progress of this field of research has been well addressed in monographs and review articles dealing with the synthesis, physico-chemical, optical properties and applications of QDs [10–12]. These reports reveal that the semiconductor nanomaterials are attractive and have interesting structures for proteome analysis with high sensitivity. Therefore, we briefly introduced on semiconductor nanomaterials and their uses as the optical probes in fluorescence spectroscopy and as affinity probes in MALDI-MS for proteome analysis.

2. Overview of Colloidal Semiconductor QDs

In 1959, R. Feynman presented a perspective lecture at Caltech, and suggested that “strange phenomena” would occur when a material’s size is reduced to nanometer scale [13]. This can cause radical changes in semiconductor nanomaterials when quantum-size phenomena (quantum confinement) take over conventional bulk properties. The semiconductor NCs or QDs are in fact artificial atoms. The smallest QDs (<1 nm) are made of ~100 atoms while the largest QDs (>20 nm) can be made from 100,000 atoms. It is confirmed that semiconductor NCs or QDs in which excitons are confined in all three spatial dimensions. This confinement can be realized by fabricating the semiconductor in very small size, typically several hundred to thousands of atoms per particle. The most striking unique property is that the absorption and emission of QDs can be “tuned” to any chosen wavelength by simply changing their size. The size of the structure limits the exciton-Bohr radius of the bound electron-hole pairs, leading to altered electronic and optical properties [14,15]. This is because their

unique size and shape-dependent optical properties are entirely different at the atomic/molecular level. Due to their discrete energy levels in both valence band and conduction band, a limited number of atoms may be present in each particle. Therefore, the absorbed energy is greater than the band gap energy, electrons (represented by the solid circle) in the valence band could absorb the energy and “jump” to the conduction band, forming short-lived electron-hole pairs and the bound state of the electron-hole pair is called an “exciton” [16]. In the quantum mechanics, this “hole” is assumed to behave as a “particle” with a certain effective mass and positive charges. Then, the electrons and holes (represented by the open circle) can quickly recombine, and photons are emitted with a specific energy corresponding to the band gap, which is the band edge emission. Therefore, charge carriers have to assume higher kinetic energies, which lead to increase in band gap and quantization of the energy levels to discrete values. This entire phenomenon is “quantum confinement effect” [17] and the theory is that behavior of exciton ensembles more like quantum mechanics of atom in 3-D model of a particle in a box [18]. Indeed, the Bohr exciton radii in bulk semiconductor QDs are approximately 3–5 nm; however, in unusual situations, the exciton size can be exceeded in the crystal dimensions by reducing particle size to a few nm. In nanometer range (1–20 nm), the physical properties of nanomaterials become very sensitive to the shape and size. The quantum size effect occurs when the size of the nanocrystal becomes comparable to or smaller than the natural length of electrons and holes. To define precisely, the Bohr radius can be utilized as a convenient length scale and the Bohr radius of a particle is given by the following equation:

$$a_B = \varepsilon \frac{m}{m^*} a_0 \quad (1)$$

where ε is the dielectric constant of the material; m^* is the reduced mass of the particle; m is the rest mass of the electron, and a_0 is the Bohr radius of the hydrogen atom [19].

Types of Semiconductor QDs

To demonstrate the related theoretical framework, we discuss the theoretical understanding of energy states for conduction electrons and their distribution related to shape and size of the materials and they are classified as the following [20].

Three dimensional system (3D): In bulk materials, carriers can freely move in all three dimensions and the material is referred as a three dimensional (3D) system. In this system, energy of the conduction electron equation is already well defined [21,22]. Similarly, quantum well can be defined that if one of the spatial dimensions of the material is in nanometer range, while the other two remain larger than the resulting structure. Quantum well is referred as a two-dimensional (2D) system since carriers are free to move in two dimensions and confined in one dimension. This 2D energy of conduction electrons is represented by the following equation.

$$E_{n_z} = \frac{\hbar^2}{8m^*} \left(\frac{n_z^2}{L_z^2} \right) + \frac{\hbar^2 k_x^2}{2m^*} + \frac{\hbar^2 k_y^2}{2m^*} \quad (2)$$

where n_z is the sub-band index. The carriers are confined in the z-dimension with thickness L_z and free in x- and y- dimensions.

The two spatial dimensions of a material are in nanometer range but the other one is larger than the resulting structure is referred as quantum wires. It is a one-dimensional (1D) system. Here, carriers are free moving in one dimension and are confined in the other two dimensions. Hence, the energy of the conduction electrons can be defined as:

$$E_{n_z} = \frac{\hbar^2}{8m^*} \left(\frac{n_z^2}{L_z^2} + \frac{n_y^2}{L_y^2} \right) + \frac{\hbar^2 k_x^2}{2m^*} \quad (3)$$

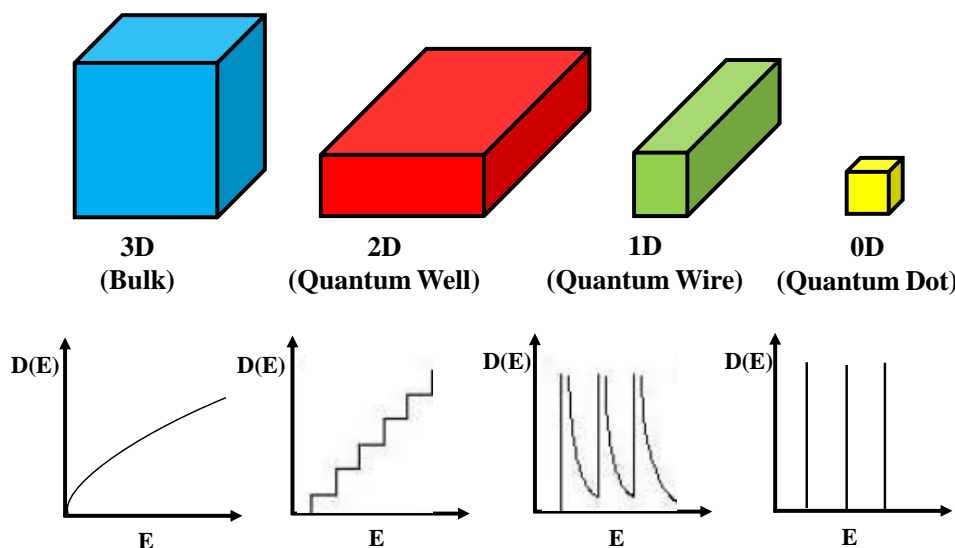
where L_y and L_z are lengths of the rectangular wire in x -, y - and z - dimensions. In this system, the energy levels depend on two quantum numbers n_y and n_z , respectively.

Similarly, quantum dot can be defined as three dimension materials are in nanometer range and it is considered to be a zero-dimensional (0D) system since carriers are confined in all three dimensions. In this system, energy levels are entirely discrete and written as:

$$E_{n_x, n_y, n_z} = \frac{\hbar^2}{8m^*} \left(\frac{n_x^2}{L_x^2} + \frac{n_y^2}{L_y^2} + \frac{n_z^2}{L_z^2} \right) \quad (4)$$

where L_x , L_y and L_z are the dimensions in x -, y -, and z - dimensions. The energy states depend on three quantum numbers n_x , n_y and n_z , respectively. The schematic diagram of density of states for 3D, 2D, 1D and 0D was shown in Figure 1.

Figure 1. Schematic diagram of density of states for 3D, 2D, 1D and 0D systems.



Furthermore, the confinement energy (the difference between the gap for low dimensional systems and 3D systems) is proportional to the size of the system. It is noticed that effective masses of charge carriers in semiconductors are less than the free electron mass, so that quantum confinement energy is observed at room temperature comparatively at a larger size (of few nanometers depending on the material) in contrast to the case of a metal, where quantum confinement energy can be observed at a low temperature only for a cluster of few atoms. Due to confinement of charge carriers, the discretization of energy levels and widening of energy gap can be realized by optical absorption and photoluminescence measurements. As a consequence of these structures, semiconductor nanomaterials were demonstrated

several altered characteristics compared to their bulk constituents. These altered physical, electronic and optical properties of semiconductor nanomaterials play key role in the development of analytical method for the analysis of proteins by fluorescence spectroscopy and MALDI-MS.

3. Semiconductor QDs-Based Fluorescence Approaches for Biomolecules Assays

One of the fundamental goals in modern proteomics is to understand the complex spatio-temporal interplay of proteins from the cellular to the integrative level. To study these interactions, the integration of unique structural characters of semiconductor QDs or NCs with analytical instruments have created many new-style tools for proteome analyses. Since, QDs have attracted broad attention to use them as optical probes for fluorescence based approaches in proteomics, which is due to their unique optical and electronic properties. Compared to organic dyes, QDs or NCs shows high quantum yield, high molar extinction coefficients (~10–100 times), broad absorption with narrow, symmetric photoluminescence spectra (full-width at half-maximum ~25–40 nm) spanning the UV to near-infrared [23]. It should be noticed that the dependence of optical properties of QDs or NCs is mainly dependent on particle size and the internal structure. It is well known that the number of surface atoms increases when the crystal size is much smaller, which can also impact the optical properties. The atoms on the surface of a crystal facet are incompletely bonded within the crystal lattice, thus disrupting the crystalline periodicity and leaving one or more “dangling orbital” on each atom pointed outward from the crystal [24]. Generally, QDs are highly faceted, and each surface contains a periodic array of unpassivated orbitals with two-dimensional translational symmetry, which may form a band structure similar to that of three-dimensional crystal itself [25,26]. If these surface energy states are within the semiconductor band gap, they can trap charge carriers at surface, thereby reducing overlap in between electron and hole, increasing the probability of nonradiative decay events. Due to their wide optical tenability, QDs have attracted broad attention in multidisciplinary science. QDs are elongated structures and emitted linearly polarized light with a wide energy separation between the absorption and emission maxima (Stokes shift). Quantum wells are well-established components of optoelectronic devices, and their colloidal “disk” analogues have recently been described, which may have novel piezoelectric applications (Reprinted with permission from Ref. [24]). These unique optical properties make them efficient optical candidates to probe the trace level biomolecules in complex samples without any sample pretreatment.

3.1. Semiconductor QDs-Based FRET and BRET Approaches

The luminescence of semiconductor QDs is very sensitive to their surface states. The fluorescence transduction is based on the principle of physico-chemical interactions between semiconductor QDs and analytes. These interactions play a key role in the efficiency of the radiative recombination, either leading to photoluminescence activation or quenching [27]. These changes can be generated by the direct interaction between the analyte and the semiconductor QDs surface, which allows the selective detection of a multitude of compounds. These mechanisms are based on energy flow (transfer of electronic excitation energy) between the components of nanoassemblies. This can occur when light energy absorbed by QDs (donor) is transferred to a nearby acceptor species, such as an

organic fluorophore (acceptor) in a process called Förster (Fluorescence) Resonance Energy Transfer (FRET) [28]. The Förster radius (R_0) can be written in Equations (5) and (6).

$$R_0^6 = \frac{900 \times (\ln 10) \kappa_p^2 \times Q_D \times I}{N_A \times 128 \times \pi^5 \times n_d^4} \quad (5)$$

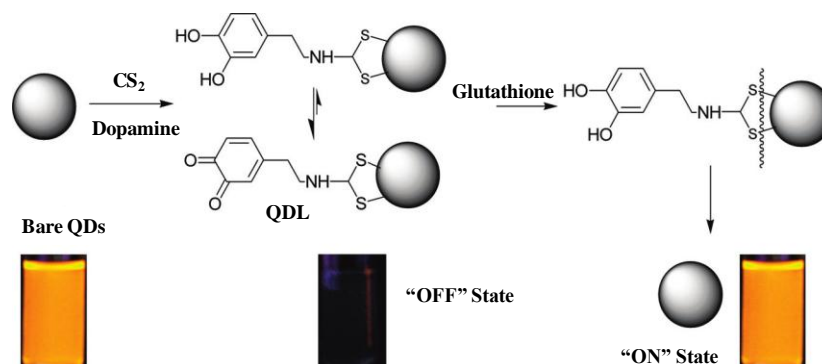
$$I = \int PL_D(\lambda) \varepsilon_A(\lambda) \lambda^4 d\lambda \quad (6)$$

where $\kappa_p^2 = 2/3$ for randomly oriented dipoles; Q_D is the quantum dot efficiency of the donor; N_A is the Avagadro's number; n_d is the reflective index of the solution; I is the spectral overlap between the donor emission and acceptor absorption and further expressed in Equation (6), in which $PL_D(\lambda)$ is the normalized emission intensity of the donor QDs, $\varepsilon_A(\lambda)$ is the absorption extinction coefficient of the acceptor and n_d is the value for water (1.333) at 580 nm. It should be noted that the rate of energy transfer depends on the distance between the donor and the acceptor, their relative orientations and the spectral overlap. Similarly, Bioluminescence Resonance Energy Transfer (BRET) is ideally suited for luminescent QDs since it avoids the difficulties in using QDs as acceptor fluorophores. BRET mechanism deals with the photon generating process to transfer the excitation energy nonradiatively to a proximal fluorescent acceptor through chemical reaction. Therefore, we will provide an overview of the literature dealing with the different semiconductor QDs-based fluorescent probes for the analysis of biomolecules by fluorescence spectroscopy.

Fluorescence "ON" and "OFF" mechanism allows us to detect biomolecules with high sensitivity and resolution. Since the resolution can be measured based on the switching of the fluorescent probes between two distinctively different fluorescent states, either fluorescent "ON" and "OFF" states or two fluorescent states with distinct color. Furthermore, the fluorescent probes must be actively varied (usually via photoswitching or photoactivation) in time to ensure that only an optically resolvable subset of fluorophores is activated at any time in a diffraction—limited region, thereby allowing their localization with high accuracy [29]. For example, Santra's group described a method for synthesis of dopamine dithiocarbamate (DDTC) capped with CdS:Mn/ZnS core/shell QDs using a water-in-oil (W/O) microemulsion mechanism [30]. These QDs acted as fluorescent probes to detect glutathione (GSH) through fluorescence ON/OFF mechanism (Figure 2). In this method, photoluminescence (PL) intensity of bare QDs was greatly quenched by the addition of DDTC, which is due to annihilation pathway by the addition of dopamine. This system was effectively allowed to detect GSH through Mn dopant-based QDs (where the ${}^4T_1 \rightarrow {}^6A_1$ Mn²⁺ ion transition is independent of QDs). It was noticed that the fluorescently dark QDs (OFF state) was observed by capping QDs surfaces with DDTC (an electron rich molecule). Interestingly, the fluorescence was restored (ON state) when the disulfide bond was cleaved by the reducing GSH. They also developed a protocol for the synthesis of water-dispersible ultra-small (3.1 nm) multifunctional CdS:Mn/ZnS core-shell semiconductor QDs and used as fluorescent probes for the bioimaging of TAT-peptide (Gyl-Arg-Lys-Lys-Arg-Arg-Gln-Arg-Arg-Arg-Gly-Tyr-Cys-NH₂)-conjugated QDs stained in brain parenchyma and blood vessels [31]. In this method, a highly water-dispersible silica layer was formed on each quantum dot (QD) by the hydrolysis and co-condensation reaction of tetraethyl orthosilicate (TEOS), 3-(aminopropyl) triethoxysilane (APTS) and 3-(rihydroxysilyl) propyl methylphosphonate (THPMP). Liu *et al.* applied thioglycolic acid (TGA) capped with CdSe/ZnS QDs as fluorescent probes to detect GSH

through OFF–ON principle [32]. They observed OFF fluorescence of QDs by adding methyl viologen; however, the QDs fluorescence was regenerated by the addition of GSH, which is due to a simple ligand displacement process between QDs and target analytes.

Figure 2. Schematic representation of quantum dots (QDs)-based fluorescence ON/OFF mechanism for the detection of glutathione. Reprinted with permission from [30].



3.2. Semiconductor QDs as Probes for Analysis of DNA, Bacteria and Cancer Cells

Shih *et al.* used 3-mercaptopropionic acid (MPA) capped with CdS QDs as fluorescent probes for sensing *Salmonella typhimurium* cells [33]. Very recently, Dutta's team used Mn²⁺-doped ZnS QDs (3–5 nm) as fluorescent probes for detecting *E. coli* [34]. The chitosan has high affinity to bind with the phosphoryl and carboxyl groups of bacterial cell wall. Due to these interactions, chitosan capped QDs can easily penetrate the bacteria cell walls. These results indicate that QDs are potential candidates to measure bacteria cells with high sensitivity. Chang *et al.* [35] synthesized biocompatible chitosan-coated ZnS QDs and chitosan-coated ZnS:Mn²⁺ QDs via a convenient one-step γ -radiation route. These QDs are well dispersed in water and used as sensors for the labeling of PANC-1 cells [35]. Similarly, Shi and Ma described the applicability of TGA capped CdS QDs as fluorescent probes for the detection of DNA molecules (DNA order 5-NH₂-GAG CGG CGC AAC ATT TCA GGT CGA-3 and a biotinylated complementarity target DNA order of 5-TCG ACC TGA AAT GTT GCG CCG CTC-3) [36]. Since the carboxylic group of TGA (negative charge) has showed high affinity to interact with amidocyanogen probe DNA (positive charge) by the electrostatic interactions. It was noticed that the PL spectrum of CdS QDs-DNA showed a little red shift when compared with TGA capped CdS QDs. The same group described that the utility of fluorescent CdS QDs for the reorganization of DNA molecules through electrostatic interactions [37]. In recent years, visible fluorescent protein constructs provide a significant data to the researchers with a tool of enormous value which can facilitate to the key identification of target molecules in cellular function in tissue sections and in living cells. Clapp's team described the application of polymer/DNA polyplexes designed water soluble QDs for gene delivery [38]. They found that increasing concentrations of pentablock copolymer and DNA led to quenching of QDs fluorescence, while chloroquine alone had no measurable effect. The designed QDs showed high affinity to monitor the dissociation of pentablock copolymer/DNA polyplexes *in vitro* and were useful for studying the release of DNA within cells.

Recently, intensive research has been carried out on QDs-based sensing probes to develop the tools for the visualization of biomolecules at a single molecule. Because of fascinating light-emitting properties, QDs are offering new exciting opportunities for modern biology to visualize cells *in vitro* and *in vivo*. Wang's group described an alternative separation-free multiplexed detection method for the detection of low abundance DNA targets, based on multicolor colocalization of target-specific QDs nanoprobe upon hybridization [39]. The designed QDs nanoprobe were successfully used for the genetic analysis of anthrax pathogenicity (*Bacillus anthracis*). Akerman's group described the applications of ZnS/CdSe QDs with three peptides (GFE-CGFECVRQCPCER; KDE-PQRRSARLSAKPAPPKPEPKP-KKAPAKK; LyP-1-CGNKRTRGC) as nanoprobe to interact with membrane dipeptidase on the endothelial cells in lung blood vessels or blood vessels and tumor cells [40]. These QDs were efficiently recognized lymphatic vessels and tumor cells in cancer related tissues. Similarly, Webb's group described the use of semiconductor CdSe/ZnSe NCs as fluorescent labels for multiphoton imaging in live animals [41]. These QDs showed high affinity to interact with target analytes for deep *in vivo* multiphoton imaging of living mice. A new class of multifunctional QDs-coated triblock copolymer (polybutyl acrylate, PBA; polyethyl acrylate, PEA; poly(methyl methacrylate), PMMA) was used for linking tumor-targeting ligands and were acted as probes for sensitive imaging of cancer cells *in vivo* conditions [42]. The designed QDs acted as nanoprobe for ultrasensitive and multiplexed imaging of molecular targets *in vivo* and allowed to detect 10–100 cancer cells. Very recently, Wu *et al.* illustrated the use of fluorescent QDs as effective probes for the improved detection and identification of *Staphylococcus aureus* directly from positive blood culture media [43]. These immunofluorescence probes were prepared by capping biotin-conjugated QDs to streptavidin-conjugated IgG molecules. QDs-IgG complex acted as binding agent to interact with a cell surface protein of *S. aureus*. It was found that 73 cultures contain gram-positive cocci in clusters and allowed the rapid identification of *S. aureus* directly from specimens. Trioctylphosphine oxide (TOPO) macrocyclic glycocluster amphiphile capped lipophilic CdSe QDs used as water soluble fluorescent sugar ball for probing of Hela cells via endocytosis [44]. The endocytic activity was depended on the sizes of sugar ball QDs, 5 nm size QDs have high endocytic activity more than that of 15 nm and 50 nm sugar ball QDs. Furthermore, Kaul *et al.* [45] described QDs-based fluorescent approach for identification of tumour cells by using labeled QDs with mortalin, and *p*-glycoprotein. These labeled QDs exhibited more photostable than the organic dyes, and allowed to localize *p*-glycoprotein with long fluorescence lifetime.

Recently, engineered QDs used as fluorescent probes for the detection of a wide variety of biomolecules [46,47]. Mattoussi's group reported the use of CdSe–ZnS core–shell QDs as bioactive fluorescent probes for imaging biomolecules [48]. In this method, lipoic acid was capped on CdSe–ZnS QDs to facilitate electrostatic conjugation of bioactive proteins. This method was successfully used as a powerful fluorescent tracking tool to identify the maltose binding protein in *E. coli*. This method was based on the electrostatic noncovalent interactions between bioconjugates of CdSe/ZnS QDs and antibodies. Goldman's group described a conjugation strategy for the attachment of antibodies to quantum dots based on the electrostatic interactions between the negatively charged dihydrolipoic acid (DHLA)-capped CdSe–ZnS core-shell QDs and positively charged proteins (natural or engineered) that serve to bridge the quantum dot and antibody [49]. The same group prepared bioinorganic conjugates luminescent semiconductor NCs (CdSe–ZnS core-shell QDs) with antibodies and used as probes in

multiplexed fluoroimmunoassays [50]. This system was successfully detected several target species including cholera toxin, ricin, shiga-like toxin 1, and staphylococcal enterotoxin B in single wells of a microtiter plate. Similarly, Chen's team developed a simple platform for the direct conjugation and separation of highly luminescent CdSe–ZnS QD–antibody complexes using a genetically engineered polyhistidine tagged elastin-protein L fusion [51]. This approach is based on the direct conjugation of QDs via metal coordination with the His tag, and showed high affinity toward IgGs and used as probes for the detection of carcinoembryonic antigen. Huang *et al.* [52] synthesized CdSe/ZnS QDs–ssDNA–fluorescent dye conjugates and used as bioprobes for the detection of micrococcal nuclease activity in the culture medium of *Staphylococcus aureus* by fluorescence microscopy. It has been reported that the QDs are conjugated with ssDNA through streptavidin-biotin affinity ligation. The ssDNA was disrupted in the presence of MNase, which digested the ssDNA.

Many researchers have described the applications of biomolecules (peptides and proteins) capped on QDs for the monitoring alterations of enzymatic activities, which plays key role in biological processes. Luminescent QDs bioconjugates are used to detect proteolytic activity by FRET [53]. Prasuhn's group functionalized QDs with dye-labeled peptides using two different linkage chemistries to yield FRET for monitoring enzymatic activity or ionic presence [54]. The QDs functionalization is based on carbodiimide chemistry through covalently link dye-labeled peptide substrates to the terminal carboxyl groups on the QD's surfaces. These QDs showed different chemistries for monitoring chemical and biological molecules. Boeneman *et al.* [55] described the use of a hybrid fluorescent protein semiconductor QDs to monitor caspase 3 proteolytic activity. In this method, mCherry monomeric red fluorescent protein was used to express an *N*-terminal caspase 3 cleavage site and it was ratiometrically self-assembled to the surface of QDs through metal-affinity coordination. The protein capped QD acted as an efficient fluorescence resonance energy transfer acceptor and allowed to monitor the proteolytic activity.

The unique photophysical properties of bioconjugated semiconductor QDs offer many advantages for active sensing, imaging and optical diagnostics [56]. Since, QDs adopted as either donors or acceptors in FRET-based assays and biosensors. Very recently, Algar's group described the utility of QDs as acceptors and donors within time-gated FRET relays [57]. In this method, the bioconjugated QDs exhibited time-gated energy transfer configuration in prototypical bioassays for monitoring protease activity and nucleic acid hybridization. These QDs also showed dual target format where each orthogonal FRET step transduced a separate binding event. Multiplexed biosensing was performed by exhibiting two approximately independent FRET mechanisms in a single QD-bioconjugate, which is due to spectrotemporal resolution of QDs-FRET without requiring multiple colors of QDs. Morgner's group reported a method on time-resolved multicolor optical analysis of FRET from a luminescent terbium complex to different semiconductor QDs [58]. This method is an efficient platform for rapid and accurate measurement on size and shape of various quantum dots under physiological conditions. It provides a new platform for the simultaneous analysis of different biological processes at sub-nanomolar concentrations. The same group described FRET mechanism between luminescent terbium complexes (LTC, as donors) to semiconductor QDs (as acceptors) for creating extraordinary large FRET efficiencies [59]. This system permits an efficient suppression of autofluorescent background which facilitates to detect analyte at sub-picomolar. Their unique physico-chemical properties make them as excellent candidates for the sensing biomolecules. The luminescent terbium complexes-QD FRET

assays confirmed that conjugated QDs have well ability to specific interaction with biotin-streptavidin or the metal-affinity coordination of histidine to zinc. Similarly, luminescent terbium complexes containing different semiconductor QDs used as probes for the multiplexed bioassay with sub-picomolar detection limits for bioanalytes [60]. Using this probe, the sensitivity of the method was greatly increased and allowed to detect single-analyte assay.

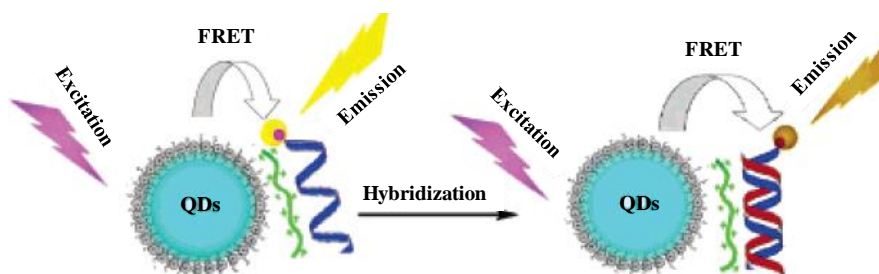
Due to their unique optical properties, semiconductors QDs have been used as central photoluminescent scaffolds for a wide variety of biosensing platforms. For example, the aptamer-capped near-infrared PbS QDs were used as a probe to detect a target protein based on selective charge transfer [61]. In this method, the water-soluble QDs were functionalized with thrombin-binding aptamer, which retains the secondary quadruplex structure for binding to thrombin. The functionalized PbS QDs were effectively interacted with thrombin with detection limit of 1 nM. This fluorescence quenching mechanism was based on charge transfer from the amine groups of protein to QDs. Similarly, quantum-dot aptamer beacons were used as fluorescence probes for sensitive detection of protein targets, such as thrombin and nucleic acid targets [62]. Rao and co-workers described the utility of CdSe/ZnS core-shell structures to identify protein-ligand interactions through BRET [63]. It was noticed that QDs were reacted with 1000 equivalents of HaloTag ligand, and then reacted with increasing concentrations of HTP-Luc8. As a result, the QDs-conjugates showed increasing bioluminescence emissions both from HTP-Luc8 and from the QDs. This approach is based on BRET where QDs act as energy acceptors for the light emitting protein (e.g., bioluminescent protein *Renilla luciferase*). The same group developed semiconductor QDs-based bioluminescence resonance energy transfer (QDs-BRET) approach for the sensing of protease activity in complex biological samples [64]. In this method, nanosensors consist of bioluminescent proteins as the BRET donor, quantum dots as the BRET acceptor and protease substrates sandwiched between the two as a sensing group. This system was successfully used to detect matrix metalloproteinases. Ma *et al.* synthesized multicolor quantum QD-encoded microspheres via layer-by-layer (LbL) assembly approach and polyelectrolyte multilayers are assembled on the QDs surfaces via electrostatic interactions [65]. In this method, two kinds of biofunctional multicolor microspheres are prepared by using two different antibodies (anti-human IgG and anti-rabbit IgG). This approach (human IgG and rabbit IgG) showed high ability to detect target antigens by the multiplexed fluoroimmunoassays.

Functionalized QDs have been widely used as fluorescent probes in the fields of biomedical and biosensing research owing to their stable and tunable multicolor fluorescence, broad absorption with narrow emission spectra, large molar extinction, high quantum yield and high chemical stability. For example, folate (FA) was attached onto the water-dispersible amphiphilic polyethylene glycol (PEG)-coated QDs (FA-PEG-QDs) via hydrophobic interactions [66]. These QDs used as fluorescent nanobioprobes for the reorganization of folate receptors (FRs) were over expressed in human nasopharyngeal cells (KB cells) but not in an FR-deficient lung carcinoma cell line (A549 cells). Similarly, Liu's group illustrated the carbodiimide coupling chemistry to prepare QDs-hydrophobic ligands through covalent modification [67]. The QDs were functionalized with a new class of hetero bifunctional ligands by incorporating different molecules such as dihydrolipoic acid, a short poly(ethylene glycol) (PEG) spacer and an amine or carboxylate terminus and subsequently attached a RhB dye to form QDs-dye conjugate FRET. These engineered QDs showed high-affinity towards target cells through covalent attachment, which facilitates to track biotinylated epidermal growth factor

(EGF) in live cells. Seeberger's group described the utility of PEGylated QDs capped with carbohydrates (D-mannose, D-galactose, and D-galactosamine) as fluorescence probes to investigate specific carbohydrate–protein interactions *in vitro* and *in vivo* in liver [68].

Recently, QDs have been functionalized with various ligands and used as fluorescent probes to detect a wide variety of biomolecules. For example, Zhang *et al.* [69] developed an ultrasensitive nanosensor platform to detect low concentrations of DNA in a separation-free format. The mechanism was based on fluorescence resonance energy transfer between QDs and the linked DNA. In this approach, QDs acts as concentrator to amplify the target signal by confining several targets in a nanoscale domain. This method was successfully used to detect a point mutation typical of some ovarian tumors in clinical samples. Similarly, Peng's group described the potential application of poly(diallyldimethylammonium chloride) (PDADMAC) capped CdTe QDs as probe for DNA-sensing [70]. This approach is based on FRET between blue-luminescent CdTe QDs and dye-labeled ssDNA (Figure 3). In this method, a cationic polymer was used as an “electrostatic linker” to achieve efficient energy transfer from the QD donor to the dye acceptor. Similarly, dodecanoic acid-(DDA)-, hexadecylamine (HAD)- and tri-*n*-octylphosphine oxide-(TOPO) capped CdSe/ZnS QDs [71] and streptavidin functionalized CdSe/ZnS and iron oxide NPs [72] have been used as fluorescent probes to identify DNA. These QDs-based fluorescence approaches allowed to detect ultra-trace target DNA within few minutes and offered the detection limit of 1.0×10^{-9} M. This platform provides a homogeneous DNA assay for fluorescence detection of DNA with minimal modification. Biomolecules were successfully functionalized on the QDs to detect bacteria. Briefly, TGA [73] and bovine serum albumin (BSA) [74] capped CdSe QDs were used as fluorescent probes for rapid detecting *Escherichia coli* and *Staphylococcus aureus*. The TGA functionalized CdSe QDs showed high degree of interaction with the amino group of bacterial cell membranes of *E. coli* and *S. aureus* and detected the bacteria at 10^2 – 10^7 CFU/mL. Similarly, BSA-conjugated CdSe QDs provided new strategy for the cell labeling with good biologically-compatible materials and this strategy was based on the interaction between BSA–CdSe or CdSe/CdS QDs and cells. The BSA-coated QDs strongly influenced the physical properties of membranes and decreased the cell membrane fluidity and the cell surface of *E. coli*. Singh's group applied TGA-capped CdSe/ZnS core/shell QDs to detect *Salmonella typhi* [75] in which the carbodiimide chemistry was utilized to conjugate *S. typhi* through carboxy terminated TGA capped QDs. This mechanism was based on the sandwich fluoroimmuno sensing between antibody immobilized membrane and bioconjugated QDs.

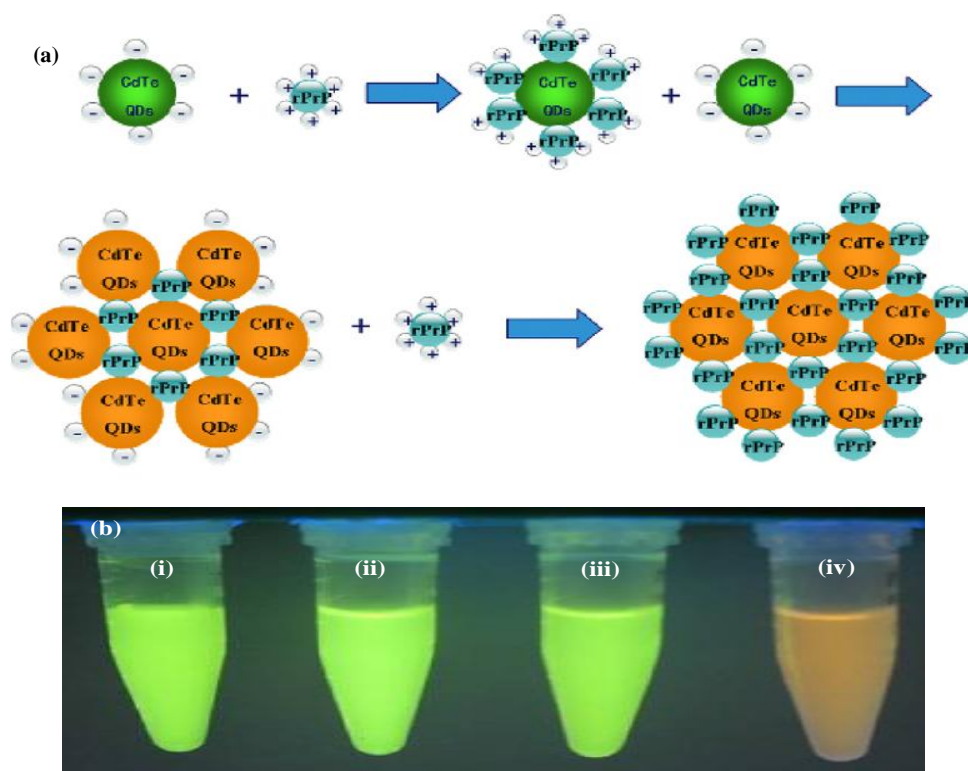
Figure 3. Mechanism of DNA hybridization-detection System based on the QDs/Cy3-labeled DNA Förster (Fluorescence) Resonance Energy Transfer (FRET). Reprinted with permission from [70].



3.3. Semiconductor QDs as Probes for Analysis of Peptides and Proteins

To efficiently enhance the specificity and sensitivity of fluorescence signal, it is necessary to functionalize QDs with organic or biomolecules to act as recognition and signal triggering elements for biomolecules assays. For example, Zheng's group prepared mercaptoacetic acid (MAA) capped CdTe QDs and used as fluorescent probes for the detection of prion protein (rPrP) [76]. These QDs showed high selectivity towards rPrP and the emission wavelengths were observed at 551 nm for original CdTe QDs and at 558 nm for CdTe QDs-conjugated rPrP, respectively. This is due to the shorter distances between the CdTe QDs in the protein conjugates than the free CdTe QDs, which can increase the dipole-dipole interaction between the CdTe QDs resulting in a larger Stoke's shift emission change (Figure 4a). The bare QDs solution emitted bright green fluorescence; however, bright green fluorescence was completely changed to orange emission by the addition of rPrP into CdTe QDs solution, which can observe with naked eye (Figure 4b). The authors studied the fluorescence abilities of CdTe QDs with various biomolecules (rPrP, BSA and His6-tagged maltose binding protein). It was found that only CdTe QDs–rPrP solution exhibited orange emission (Figure 4b).

Figure 4. (a) Interactions of CdTe QDs with rPrP; (b) Colorimetric qualitative detection of rPrP ($6.7 \mu\text{g mL}^{-1}$) with CdTe QDs ($1.0 \times 10^{-6} \text{ mol L}^{-1}$). The excitation wavelength of UV lamp was 302 nm. (i) CdTe QDs; (ii) CdTe QDs with BSA; (iii) CdTe QDs with His6-tagged MBP and (iv) CdTe QDs with rPrP. Reprinted with permission from [76].



The applications of QDs are vastly diverse with tremendous outcome in multidisciplinary research. Many QDs have been functionalized with various capping agents to sensor proteins. For instance, citrate- [77] and diethanolamine- [78] capped CdSe QDs were used as fluorescent probes to detect cytochrome c, hemoglobin, myoglobin and BSA. The CdSe and CdSe/CdS have well-defined 1s–1s

electron transitions and the fluorescence intensity of cytochrome c (2×10^{-9} M) was significantly quenched by the exposure of CdSe/CdS core-shell QDs. This quenching mechanism was based on the photo-induced electron transfer between QDs and cytochrome c because it is an electron transfer protein. Similarly, the flower-like CdSe nanostructure particles were used as fluorescent probes to detect BSA [78]. CdSe QDs fluorescence intensity was strongly quenched by the interaction of CdSe QDs with tryptophan residues. The BSA structure was greatly changed by interaction with CdSe QDs. It is a static quenching phenomenon between the quencher (CdSe QDs) and the fluorophore (BSA). CdSe/ZnS core-shell QDs were used as optical sensors to investigate optical and structural properties of QDs conjugated with BSA [79]. Curri's group modified the procedure for preparation of CdSe/ZnS core-shell with hydrophobic ligands (DSPE-PEG-2000—1,2-distearoyl-sn-glycero-3-phosphoethanolamine-N-[carboxy(polyethylene glycol)-2000]) [79]. The functionalized CdSe/ZnS QDs showed strong tendency to interact with BSA through amide bond between functionalized QDs/PEG lipid micelles and the primary amine groups of the BSA. These BSA conjugated QDs can be used as optical probes for multi-color and multiplexing bio-probes detection and also can be used for molecular recognition processes. Furthermore, the TGA-coated CdTe QDs were used as fluorescent probes to study the optical properties of BSA [80]. This conjugation is based on the electrostatic interactions between the carboxylic group of TGA with the amino group of BSA. It was noticed that the fluorescence intensity of QDs was gradually increased with the increasing amount of BSA. To quench the fluorescence intensity, three surfactants were added into the QDs-BSA conjugated system. The maximum quenching efficiency was observed in the presence of cetyltrimethylammonium bromide (CTMAB). This method demonstrated the high performance QDs-NR FRET sensor for ultra sensitive detection of target species with low background signals. To increase the fluorescence quenching, He's team prepared TGA-coated CdTe QDs (2–3 nm) and used as optical probes to study the interactions between CdTe QDs and chymotrypsin by UV-visible, fluorescence and resonance Rayleigh scattering tools [81]. It was obvious that CdTe QDs successfully quenched the intensity of chymotrypsin at pH 7.2 via static quenching. The same group described the application of 2-mercaptoethylamine (MEA) capped CdTe QDs as fluorescent probes to investigate QDs interactions with human serum albumin (HAS) [82]. The fluorescence intensity of HSA was strongly quenched by the addition of CdTe QDs due to the electrostatic interactions between the positive charge of MEA-CdTe QDs and the negative charge of HSA.

Very recently, Jiang's and Liu's teams synthesized CdTe QDs with different ligands such as mercaptopropionic acid (MPA), N-acetylcysteine (NAC) and GSH used as optical probes to investigate the HSA structures by using fluorescence spectroscopy, circular dichroism (CD), UV-vis spectroscopy and dynamic light scattering [83]. In this method, both the static and dynamic quenching mechanisms occurred through electrostatic interactions between QDs and HSA. Wei's group investigated the influence of CdTe QDs size on the toxic interaction with HSA [84]. In this method, two aqueous-compatible CdTe QDs with maximum emission of 535 nm (green-emitting QDs, G-QDs, 2.04 nm) and 654 nm (red-emitting QDs, R-QDs, 3.79 nm) were used and it was concluded that the quenching effect of QDs on HSA fluorescence depended on the size. They confirmed that the nature of quenching is not dynamic but probably static, resulting in forming QDs-HSA complexes. Similarly, Huang's and Liu's groups prepared MPA capped CdTe QDs and used as fluorescent probes for the investigation of optical properties of HSA using fluorescence spectroscopy [85]. In this method, four

sizes of MPA capped CdTe QDs with maximum emission of 520 nm (green QDs), 568 nm (yellow QDs), 620 nm (red QDs) and 680 nm (crimson QDs) were studied and found that the quenching of HSA fluorescence intensity is QDs size-dependent relationship. This quenching is based on the electrostatic interaction between QDs and HSA, which facilitate to form QDs–HSA complex. It was noticed that the biological activity of HSA was very poor at bigger sizes of QDs. Wang's and Liu's teams studied the interaction of CdTe QDs coated with MPA, L-cysteine, and GSH with BSA by fluorescence, UV–vis absorption and circular dichroism [86]. The functionalized CdTe QDs effectively quenched the fluorescence intensity of BSA and the interactions were based on the electrostatic interactions, which results to form QDs-BSA complexes. These results play a key role to understand QDs-proteins interactions in proteomics.

Recently, several fluorescent semiconductor QDs have been synthesized and applied as fluorescent probes in proteomic studies. Briefly, L-cysteine-capped ZnS [87] and MAA-capped ZnSe [88] QDs were used as fluorescent probes for analysis of several proteins by fluorescence spectroscopy. The fluorescence intensity of L-cysteine capped ZnS QDs was increased by the addition of proteins such as BSA, HSA, γ -globulin, ovalbumin at 267 nm in pH 5.12 [87]. Similarly, the fluorescence intensity of MAA capped ZnSe QDs was greatly enhanced by the addition of BSA at pH 7.0 and the limit of detection was 0.06 nM [88]. The fluorescence intensity of QDs was enhanced by the presence of BSA and emitted a characteristic peak at 348 nm. As a result, strong interactions occurred between the functionalized ZnSe with BSA. Furthermore, *p*-sulfonatocalix[4,6]arene could be used as a stable ligand to prepared water-soluble nanoparticles via chemical bonding. As a result, Li and co-workers described a simple procedure for the preparation of highly fluorescent, stable and water-soluble CdSe QDs functionalized with *p*-sulfonatocalix(*n*)arene (SFCA, *n* = 4 or 6) and used as fluorescent probes for the detection of aminoacids [89]. It was found that the SFCA(4) coated CdSe QDs showed high selectivity towards methionine, similarly, SFCA(6) coated CdSe QDs showed high affinity towards phenylalanine. The fluorescence signal intensity of SFCA(*n*) coated with QDs was greatly enhanced in the presence of methionine and phenylalanine. Based on the above reports, we assert that the surface of QDs needs to be altered to the increase stability and allow conjugation of biomolecules for specific targeting. Table 1 indicates the semiconductor QDs-based fluorescence spectrometric methods for the analysis of biomolecules.

Table 1. Detection of biomolecules using semiconductor QDs-based fluorescence spectroscopic methods.

Name of QDs	Name of the ligand	Diameter (nm)	Analytes	Detection limit (nM)	Reference
CdS:Mn/ZnS	DDTC	5	GSH	-	[30]
CdS:Mn/ZnS	Amine group	3.1	TAT-peptide	-	[31]
CdSe/ZnS	TGA	-	GSH	-	[32]
CdS	MPA	2–5	<i>Salmonella typhimurium</i> cells	-	[33]
Mn ²⁺ ZnS	Chitosan	3–5	<i>E. coli</i>	-	[34]
Mn ²⁺ ZnS and ZnS	Chitosan	4.5	PANC-1 cell	-	[35]

Table 1. Cont.

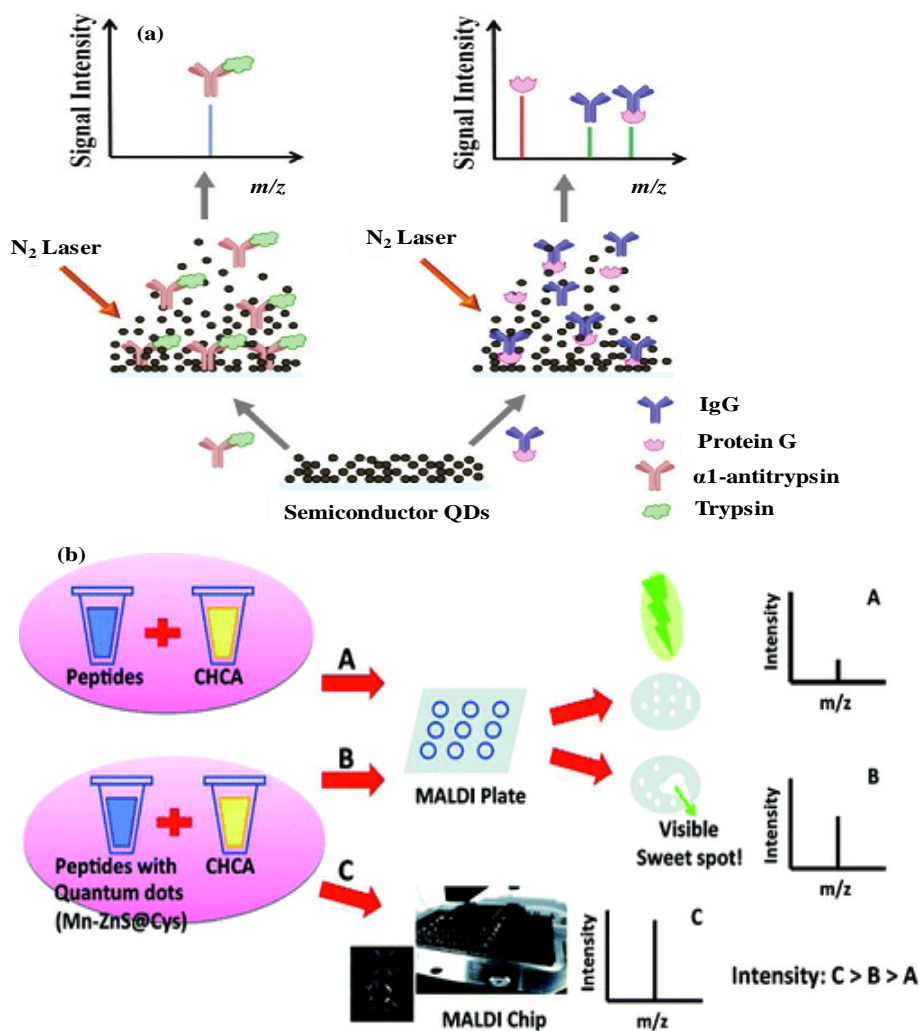
Name of QDs	Name of the ligand	Diameter (nm)	Analytes	Detection limit (nM)	Reference
CdS	TGA	5	DNA	-	[36]
CdSe/ZnS	Peptides (GFE, KDE, LyP-1)	<10	Tumors	-	[40]
CdSe/ZnS	PBA, PEA, PMMA	2.5–5.0	Cancer cell	10–100	[42]
CdSe	TOPO-sugars	5–50	Hela cell	-	[44]
CdSe/ZnS	FA-PEA-PEG-750	13	KB vs. A549 cells	-	[66]
CdSe/ZnS	Amino, carobxy and hydroxy groups PEG	-	Hela cell	-	[67]
CdSe/ZnS	PEG- D-mannose, D-galactose, and D-galactosamine	15–20	Hepatocellular carcinoma cell line HepG2	-	[68]
QDs	Streptavidin	-	DNA	4.8×10^{-15}	[69]
CdTe	PDADMAC	-	DNA	-	[70]
CdSe/ZnS	TOPO-DDA, TOPO-HDA	3.3	DNA	$<1.0 \times 10^{-9}$	[71]
CdSe/ZnS and iron oxide NPs	Streptavidin	30	DNA	5.0×10^{-6}	[72]
CdSe	TGA	3–4	<i>E. coli</i> and <i>S. aureus</i>	10^2 CFU/mL	[73]
CdSe	BSA	5	<i>E. coli</i> (HB101)	-	[74]
CdSe/ZnS	TGA-IgG	6	<i>Salmonella typhi</i>	10^2 cells/mL	[75]
CdTe	MAA	~3.4	rPrP, <i>E. Coli</i> cytochrome c, hemoglobin and myoglobin	3.0	[76]
CdSe and CdSe/CdS	Citrate	-	BSA	-	[77]
CdSe	Diethanolamine	20	BSA	-	[78]
CdSe/ZnS	DSPE-PEG-2000	3.5–4	BSA	-	[79]
CdTe	TGA-neutral red-BSA	3.1	BSA	1.97	[80]
CdTe	TGA	2–3	Chymotrypsin	-	[81]
CdTe	MEA	-	HSA	4.2	[82]
CdTe	MPA, NAC, GSH	-	HSA	-	[83]
CdTe	MPA	2–4.8	HSA	-	[85]
CdTe	MPA, L-Cys, GSH	3.5	BSA	-	[86]
ZnS	L-Cys	17	BSA, HSA, γ -globulin, ovalbumin	0.06–0.56	[87]
ZnSe	MAA	25	BSA	30.3	[88]
CdSe	SFCA ($n = 4, 6$)	-	Methionine and phenylalanine	3000–4000	[89]

4. Semiconductor Nanomaterials-Based MALDI-MS for Biomolecules Analysis

In MALDI-MS, the organic matrices such as 2,5-dihydroxybenzoic acid (DHB), α -cyano-4-hydroxycinnamic acid (CHCA) and sinapinic acid (SA) act as energy mediators for laser absorption and transferring of laser energy to target analytes for their desorption and ionization, which minimize the analytes damage and fragmentation from laser irradiation. Generally, a good matrix exhibits good ability to form co-crystallization with target analytes, which leads to generate a layer of

small crystals. By applying nitrogen (N_2) laser at 337 nm, the analytes get evaporate and leads to create gas phase ions and then can be identified by mass spectrometry (Figure 5a). Although organic matrices acted as potential candidates for analyzing large biomolecules (peptides and proteins) by MALDI-MS, there are some problems associated with the use of organic matrixes such as strong interference at low mass region and inability to enrich trace level target molecules. Since the organic matrices typically form heterogeneous crystallization to create “sweet spots”, resulting in poor shot-to-shot and sample-to-sample reproducibility. Recently, various types of nanomaterials have been applied in MALDI-MS for the analysis of a wide variety of molecules. Since, nanomaterials have large surface areas for large analyte loading capacity (e.g., >1000 small molecules per single nanoparticle), and surface chemistry of nanomaterials allows us to act as affinity or concentrating probes for the enrichment or preconcentration of target molecules in biocomplex samples (Figure 5b). Because the number of adsorbed analytes can be increased with decreasing size of nanomaterials, greater desorption/ionization efficiency with higher sensitivity is provided.

Figure 5. (a) Schematic representation of QDs as matrices for analysis of biocomplex structures by laser desorption ionization (LDI)-MS. Reprinted with permission from [90]; (b) Schematic diagram of peptide analysis by using hydroxycinnamic acid (CHCA), QDs along with CHCA and QDs based matrix-assisted laser desorption/ionization (MALDI) chip along with CHCA. Reprinted with permission from [91].

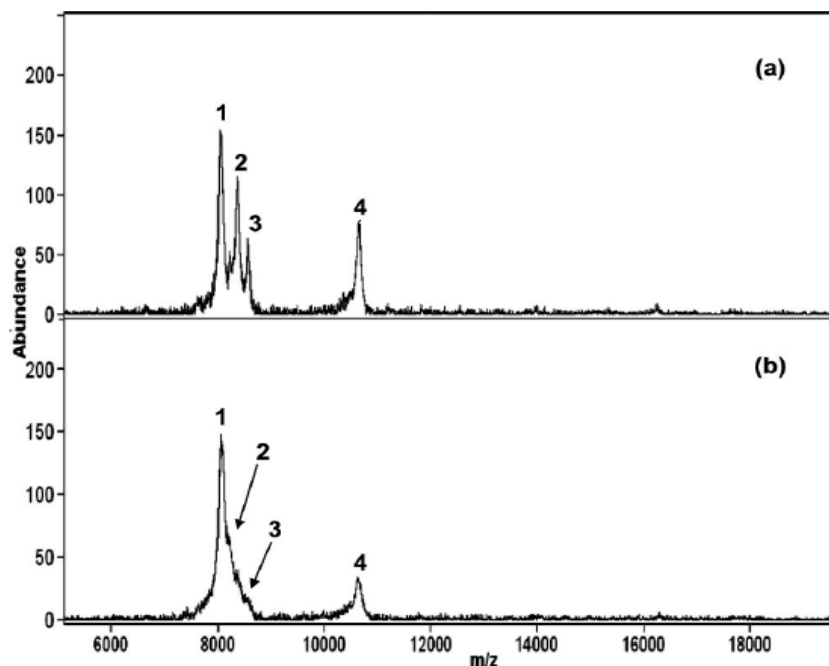


Tanaka's group first demonstrated the potential use of cobalt powder (30 nm) dispersed in glycerol as the inorganic matrix for the analysis of proteins by MALDI-MS [92]. Nanomaterials surfaces exhibit several unique properties such as higher analyte loading capacities, high molar absorption coefficients, efficient absorption of laser light, minimal degree of fragmentation with reduced background noise and high affinity to enrich target species from sample solutions. In recent years, scientific interest towards the chemistry of semiconductor nanomaterials have been rapidly grown in multidisciplinary research areas and successfully integrated with mass spectrometric tools for the analysis of biomolecules [93]. Since nanomaterials integrated MALDI-MS possesses distinctive advantages such as sensitivity, enrichment of trace amounts of targets and minimization of sample pretreatment procedures to the biomolecules assays [94,95]. In response to these advantages, a variety of nanomaterials including metal and metal oxide nanoparticles, semiconductor nanoparticles and QDs have been introduced as matrices and affinity probes for the efficient analysis of biomolecules by MALDI-MS. However, this review provides a general overview of recent approaches on semiconductor nanomaterials-based MALDI-MS for the analysis of biomolecules.

4.1. Metal Sulphide Semiconductor NMs-Based MALDI-MS

Due to their unique physico-chemical properties, semiconductors-based nanomaterials have been intensively used in MALDI and matrix-less laser desorption ionization (LDI) mass spectrometry; the ultimate objective is to overcome several serious limitations (reproducibility, enrichment of trace level analytes, and elimination of background noise) intrinsically related to the use of conventional organic matrices in MALDI-MS [93–95]. Therefore, Wu's group introduced various functionalized semiconductor nanomaterials and used as matrices, affinity probes and heat absorbing probes for the analysis of peptides, proteins and bacteria by LDI- and MALDI-MS [96–105]. Briefly, the ZnS NPs were functionalized with five different functional groups (MPA, sodium citrate, cysteamine, and 2-mercaptoethane sulfonate) and used as affinity probes for the analysis of proteins by MALDI-MS [96]. It was noticed that MPA functionalized ZnS NPs were effectively acted as affinity probes to concentrate ubiquitin-like proteins from oyster mushroom (*Pleurotus ostreatus*). In this approach, MPA capped ZnS NPs have showed high affinity towards ubiquitin-like proteins (Figure 6). Similarly, azide capped ZnS-N₃ NPs used as separating and affinity probes (separation-/washing free) to isolate/concentrate milk proteins and ubiquitin like proteins from oyster mushroom prior to their identification by MALDI-MS [97]. The separation and preconcentration phenomenon was based on the electrostatic interaction between ZnS-N₃ NPs surfaces and proteins. Because of their inherent advantages, Mn²⁺-doped ZnS NPs functionalized with cysteine and used as matrix for the analysis of small molecules [98]. Since, Mn²⁺-doped ZnS NPs have potentiality to absorb a greater number of molecules on their surfaces over those of traditional organic matrixes, which facilitates to generate more number of analytes desorption/ionization from NPs surfaces per laser shot, offering a greater sensitivity.

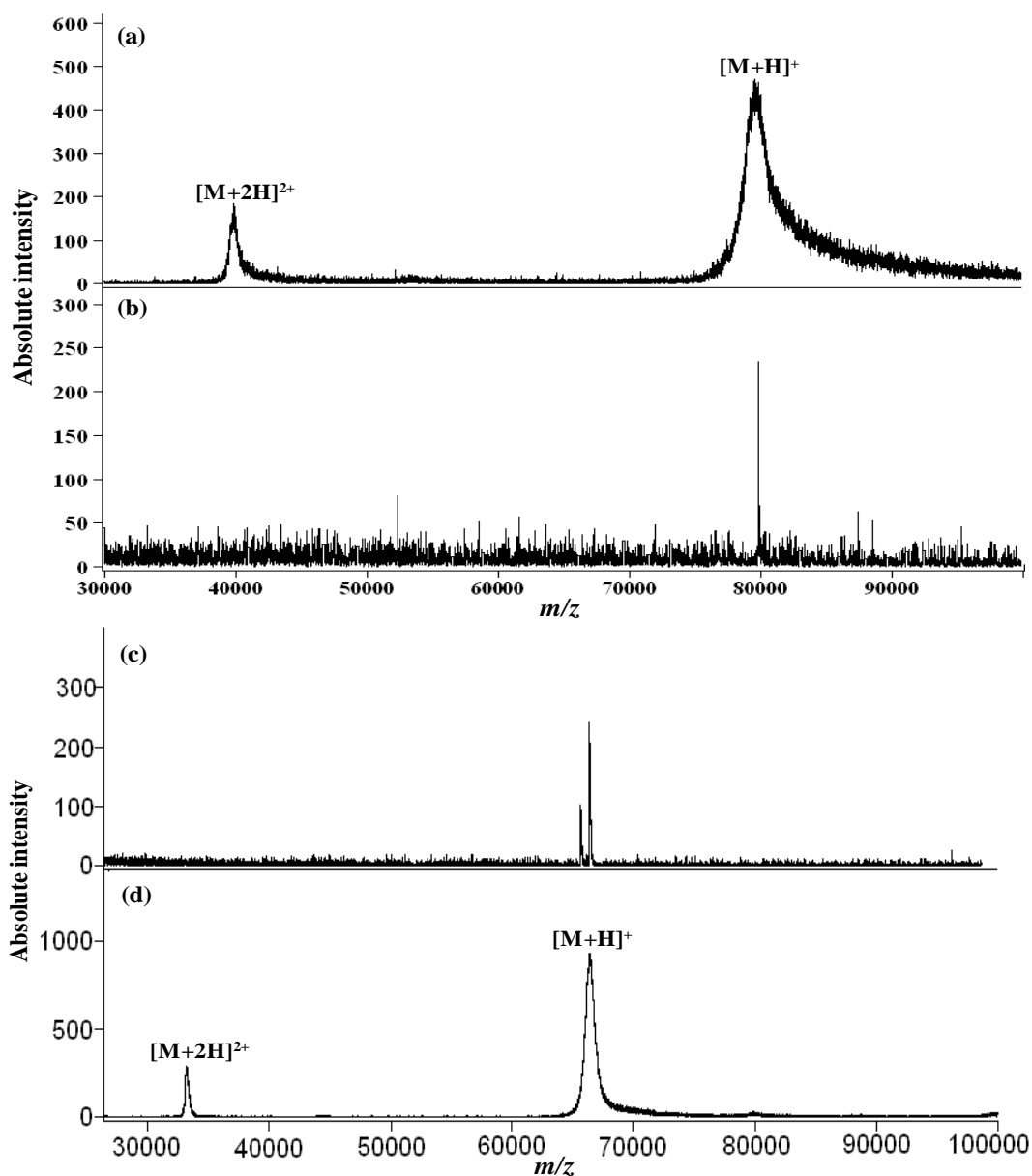
Figure 6. MALDI-mass spectra of ubiquitin-like proteins in oyster mushroom by (a) ZnS-MPA NPs as the matrix and affinity probes; and (b) sinapic acid (SA) as the matrix. Peaks 1, 2, 3, and 4 at m/z 8063, 8384, 8593, and 10 666 are attributed to the ubiquitin-like protein (8.0 kDa), ubiquitin-like protein (8.3 kDa), ubiquitin (8.5 kDa), and ubiquitinlike protein (10.5 kDa), respectively. Reprinted with permission from [96].



Semiconductor CdS QDs and NPs functionalized with MPA [99,100] and 4-aminothiophenol (ATP) and 11-mercaptopundecanoic acid (MUA) [100] and used as matrices and affinity probes for the analysis of biomolecules by MALDI- and ESI-MS. The MPA capped CdS QDs were covalently interacted with large proteins and the mass resolution of large proteins (bovine serum albumin, human serum albumin and transferrin, 66,000–80,000 Da) was greatly enhanced by acting as efficient energy mediators (Figure 7). Furthermore, MPA capped CdS QDs used as affinity probes for the enrichment of microwave digested proteins (cytochrome c and lysozyme) prior to their identification by ESI-MS [100]. Semiconductor CdS NPs capped with ATP and MUA used as matrices and as co-matrices for the analysis of peptides and proteins in MALDI-MS [101]. It was observed that the $-NH_2$ group of ATP and $COOH$ group of MUA on CdS NPs acted as a supporting matrix for the efficient transfer of protons to target analytes during their desorption/ionization. Using these materials, peptides and proteins signals were generated with high signal intensities with reduced background noise and increased mass resolution (4–13 folds). These ATP- and MUA- capped CdS NPs used as affinity probes to isolate/concentrate hydrophobic proteins (soybean hydrophobic protein, soybean Bowman–Birk proteinase inhibitor and soybean inhibitor D-II) in soybean prior to their identification by MALDI-MS. The potential of MUA capped CdSe QDs-assisted LDI-MS as a new tool for proteomic studies [102]. The functionalized CdSe QDs acted as an effective probe to interact with biomolecules through covalent interactions. This method greatly enhanced the signal intensities of proteins and the LOD of peptides was found to be 100 pM. Importantly, the MUA capped CdSe acted as concentrating probes in the presence of signal suppressors such as urea and Triton X-100. Multiwalled carbon nanotubes doped with Cd^{2+} ions and modified with CdS NPs used as affinity probes

for the analysis of peptides and microwave-digested proteins in the atmospheric pressure matrix-assisted laser desorption/ionization (AP-MALDI) and MALDI MS [103]. Moreover, these NPs also acted as heat-absorbing materials for efficient microwave tryptic digestion of cytochrome c and lysozyme in MALDI-MS.

Figure 7. MALDI—mass spectra of transferrin using (a) SA; and (b) CdS QDs as the matrices. MALDI—mass spectra of bovine serum albumin (BSA) using (c) CdS QDs; and (d) SA as the matrices. Reprinted with permission from [99].



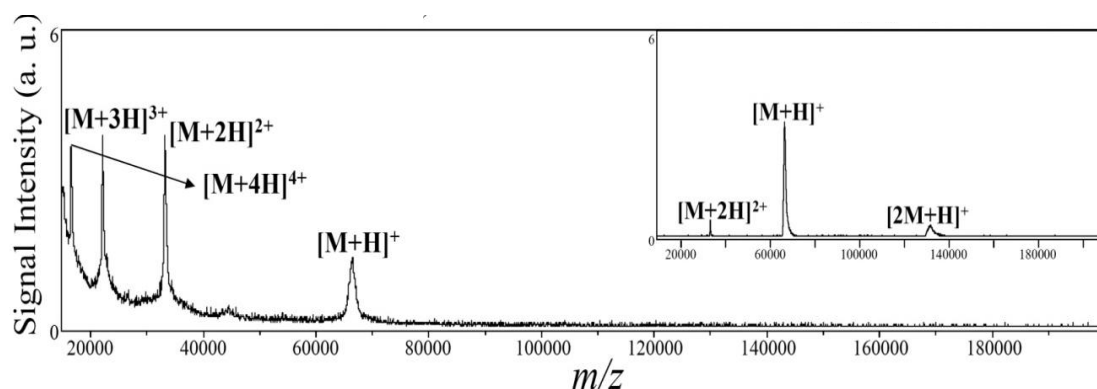
4.2. Metal Selenide, Telluride and Oxide Semiconductor NMs-Based MALDI-MS

Furthermore, MPA capped ZnSe QDs were used as the matrix and affinity probes for direct analysis of peptides and proteins from sodium salt solution in SALDI-MS [104,105]. The signal enhancement was owing to the electrostatic interaction between QDs and biomolecules, which facilitate the

adsorption proteins onto the surfaces of ZnSe QDs. Using this method, several biomolecules such as Leu-enk, Met-enk, HW6, substance P and angiotensin II, cytochrome c, myoglobin and lysozyme were successfully analyzed by MALDI-MS. Moreover, these approaches provided straightforward tool for the identification of peptides, proteins and digested proteins with reduced sample preparation procedures. It is well known that the organic matrices can create invisible “sweet spots” that are formed during heterogeneous cocrystallization which can minimize the analytical throughput and affect the reproducibility of MALDI-MS. To solve this problem, Lai’s group described the potential applications of cysteine capped Mn^{2+} -ZnS QDs-assisted MALDI-MS for peptide and protein analysis [91]. These functionalized QDs NPs acted as affinity probes for selective trapping of target biomolecules through strong interactions between analytes and the cysteine capping agents on the surfaces of QDs. Due to their small size and high surface-to-volume ratio, biomolecules are strongly adsorbed on the surfaces of QDs, which can increase relative peptides concentration. Importantly, Mn^{2+} -ZnS QDs acted as nucleation centers for the formation of visible sweet spots during matrix crystallization and permitted to enhance the signal intensities of target molecules at 1.0 pM. Similarly, Chang *et al.* [90,106] reported the tremendous applications of HgTe nanostructure materials as matrices and affinity probes for the analyses of large proteins complexes (150,000 Da) (Figure 8). In these methods, several influencing parameters such as nanostructure, surfactant, pH and salt concentrations were investigated for the analysis of large proteins by SALDI-MS with high sensitivity. It was observed that BSA protein signals were generated by using ammonium citrate (pH 5.0). Due to their weaker interaction (BSA (pI 4.5) and HgTe nanostructures (zeta potential, -37.6 mV)), efficient desorption occurred for the generation of large proteins signals. Apart from this, HgTe nanostructure acted as concentrating probes, which facilitated to decrease LODs by a factor of all most 50 times [90]. Similarly, they also described the use of MPA capped HgTe nanostructures as the matrix for the analysis of large proteins (α 1-antitrypsin, trypsin, IgG, protein G) and their complexes by SALDI-MS [106]. They studied the role of several surfactants (PEG 300, PEG 600, PEG 2000, Tween 20, Brij 30, Brij 35, Brij 56, and Brij 76, 1%) for the detection of protein-protein complexes by SALDI MS. It was noticed that only Brij 76 was provided the best conditions for the detection of protein-protein complex ions $[\alpha_1\text{-antitrypsin+trypsin+H}]^+$ at m/z 72,160. This is due to Brij 76 surfactant has high hydrophobicities (nonpolar alkyl chains and OH groups), which allow to stabilize the protein-protein complexes. Using this method, the interactions of IgG and protein G proteins were investigated and the signals were observed at m/z 74,885, 49,984, 26,023, 13,019, 86,585, and 58,297 corresponding to $[\text{IgG} + 2\text{H}]^{2+}$, $[\text{IgG} + 3\text{H}]^{3+}$, $[\text{protein G} + \text{H}]^+$, $[\text{protein G} + 2\text{H}]^{2+}$, $[\text{IgG} + \text{protein G} + 2\text{H}]^{2+}$, and $[\text{IgG} + \text{protein G} + 3\text{H}]^{3+}$ adducts, respectively. This HgTe-based SALDI-MS allowed to detect protein G (m/z 26,023) and IgG (m/z 149,931) at 2 μM (1 pM) and 5 μM (2.5 pM) with ease sample preparation at minimal sample volume. Very recently, Kailasa and Wu described that the potential applications of DDTC capped QDs [107] and the bare BaTiO_3 NPs [108] as affinity probes for the enrichment of microwave tryptic digest proteins (cytochrome c, lysozyme and BSA and phosphoproteins) prior to MALDI-MS analysis. Using QDs as affinity probes, proteolytic peptides of amino acid sequence coverages were observed with 92%, 75% and 56% for cytochrome c, lysozyme and BSA, respectively [107]. Similarly, BaTiO_3 NPs-assisted MALDI-MS provides higher digestion efficiency and enriched maximum number of phosphopeptides from the tryptic digest phosphoproteins [108]. Overall, these approaches provided rapid tools for digestion of proteins (50 s) and effectively

trapped/enriched proteolytic peptides in 30 min, which is promising for automated high-throughput proteomics studies in modern biology.

Figure 8. Mass spectrum of BSA (5 μ M) recorded using a matrix of HgTe nanostructures prepared in 300 mM ammonium citrate (pH 5.0). The signals at m/z 66 431, 33 216, 22 144, and 16 609 represent the adducts $[M + H]^+$, $[M + 2H]^{2+}$, $[M + 3H]^{3+}$, and $[M + 4H]^{4+}$, respectively. Inset: Mass spectrum of BSA obtained in SA matrixes (20 mg/mL in water/ACN (1:1, v/v) containing 0.1% TFA). The signals at m/z 132 862, 66 431, and 33 216 represent the adducts $[2M + H]^+$, $[M + H]^+$, and $[M + 2H]^{2+}$, respectively. Reprinted with permission from [90].



Xiong's group described a new method for the synthesis of SnO_2 -poly(methyl methacrylate) (PMMA) and TiO_2 -PMMA core-shell nanobeads and used as affinity probes to concentrate intact horse heart myoglobin (400 nm) and trypsin-digested myoglobin peptides (1 nm) prior to SALDI-MS [109]. The SnO_2 -PMMA nanobeads showed the superior qualities to concentrate and enrich target analytes in SALDI MS than that of TiO_2 -PMMA. Since, SnO_2 NPs (2 nm) have smaller size than TiO_2 NPs (8 nm), which permits higher capacity to trap/concentrate proteins from the brain of Sprague-Dawley rat. Chang's [110] team described the utility of six nanomaterials (Au, TiO_2 , Se, CdTe QDs, Fe_3O_4 , and Pt nanospheres) as matrices for the analysis of glutathione, angiotensin I, insulin, cytochrome c and chymotrypsin by SALDI-MS. Large protein (cytochrome c) signals were generated with a greater number of adducts using Fe_3O_4 NPs and CdTe QDs as SALDI substrates because Fe ions desorbed and ionized from the NPs than those from the mixtures of the metal ions. The limit of detection was 5.6 fM for cytochrome c using Fe_3O_4 NPs as the matrix. Based on these results, we assert that NPs need to meet the three criteria such as (i) high ability to absorb the laser energy; (ii) prevent analyte aggregation and well co-crystallization; and (iii) provide a source of charging (e.g., H^+). Therefore, these semiconductor nanomaterials-based MALDI-MS approaches offer a powerful bioanalytical tool for ultra-fast analysis of trace level proteins.

4.3. Semiconductor Nanomaterials-Based MALDI-MS for Bacteria Analysis

To enhance the specificity and sensitivity of the bacteria proteins signals, it is necessary to seek suitable methods for the functionalization of NPs with organic or biomolecules as affinity probes and signal triggering elements. To improve the signal intensities of bacteria proteins, our group published a series of papers on NPs-assisted MALDI-MS for the analysis of bacterial proteins in various bacteria

species [111–116]. Several nanomaterials such as $\text{Mg}(\text{OH})_2$ [111], ZnO [112,113], CdS QDs [114], TiO_2 [115], and titanium-based biochip [116] have been used as affinity probes/concentrating probes for the enrichment of bacteria proteins prior to MALDI-MS analyses. In these approaches, oleic acid capped $\text{Mg}(\text{OH})_2$ NPs were used as extracting and concentrating probes for the enrichment of hydrophobic proteins in *E. coli* before their identification by MALDI-MS [111]. Similarly, ZnO NPs [112] acted as affinity probes for the analysis of bacteria proteins in *E. coli* [112] and in *Staphylococcus aureus* [113]. The degradative ability of CdS QDs was investigated on extracellular polysaccharides of *E. coli* cells [114]. Similarly, TiO_2 NPs-assisted MALDI-MS used as a biosensor for the detection of clinically important bacterium (*Staphylococcus aureus*) in air, nasal passage and skin samples [115]. It was noticed that the bacteria signals were significantly improved and several mass peaks from the nasal and air samples were identical with the standard *S. aureus* peaks. To improve the detection ability and sensitivity for bacteria species, titanium bacterial chip-based MALDI-MS was used as biosensor for the sensitive detection of pathogenic bacteria such as *Staphylococcus aureus subsp. aureus* and *Pseudomonas aeruginosa* [116]. Using this approach, bacteria was detected at $<10^3$ cfu/mL. Our group also described the enrichment of peptides and proteins using ZrO_2 and $\text{ZrO}_2\text{-SiO}_2$ NPs [117] and bare TiO_2 , TiO_2 -dopamine and TiO_2 -CdS [118] by MALDI-MS. The target analytes were effectively trapped and the concentrated target analytes (Leu-enk, Met-enk, thio peptide (thio) and angiotensin I and II (Angio-I and -II) and milk proteins) from the biocomplex samples through electrostatic [117] and covalent interactions [118] between nanomaterials and target analytes. These approaches provide efficient platforms for sensitive analysis of peptides and proteins (5–11 folds). Using this approach [117], several milk proteins were selectively isolated/concentrated from non-fat milk and the mass peaks at m/z 9,430, 11,489, 11,710, 14,173, 18,160, 18,975, 20,051, 23,574, 23,982 and 25,178 corresponded to proteose peptone PP81, γ_3 -casein, γ_2 -casein, α -lactoalbumin, β -lactoglobulin, κ -casein, γ_1 -casein, α_{s1} -casein, β -casein, and α_{s2} -casein, respectively were detected. Very recently, we described the dual application of 12-hydroxy octadecanoic acid (HOA)-modified barium titanate nanoparticles (BaTiO_3 NPs) in MALDI-MS for the analysis of phospholipids (PLs; L-A-phosphatidyl-l-serine (PS) and L-A-phosphatidic acid sodium (PA)) and hydrophobic proteins in *E. coli* [119]. This method showed good linearity in the concentration ranges of 1.0–5.0 μM and 1.0–10.0 μM for PS and PA, respectively. The HOA-modified BaTiO_3 NPs-assisted LLME coupled with MALDI-MS was successfully detected several hydrophobic proteins (membrane proteins—*ecnB* (P56549), *lpp* (P69776), and *osmE* (P23933); hypothetical membrane proteins—*yifL* (P39166) and *ygdI* (P65292); acetyl-acyl carrier protein (*ydhI*; *acetyl-ACP*, P0A6A8) and lipoproteins (*ecnB*, *lpp*, *osmE*, *yifL*, *ygdI*) and water-insoluble ATPase proteolipid (at m/z 8282; *atpL*, P68699)) in *E. coli*. It proved as a simple sample pretreatment for efficient extraction, preconcentration of hydrophobic proteins in biological samples prior to MALDI-MS analysis. These approaches proved as an alternate method to use sample cleanup method, which is promising either selective extraction of the desired analytes or selective rejection of interfering species. Table 2 shows the overview of semiconductor nanomaterials-based MALDI-MS for the biomolecules assays. Therefore, functionalized semiconductor nanomaterials-based MALDI-MS approaches are promising platforms for the efficient extraction and enrichment of trace level target species in biocomplex samples.

Table 2. Overview of semiconductor nanomaterials-based MALDI-MS for biomolecules assays.

Name of semiconductor NPs	Capping ligand	Analytes	Size (nm)	Detection limit	Technique	Reference
ZnS	MPA	Insulin, ubiquitin	-	85–91 nM	MALDI-MS	[96]
ZnS	N ₃	Milk and ubiquitin-like proteins	15	-	MALDI-MS	[97]
CdS	MPA	Peptides and proteins	5	-	LDI-MS	[98]
CdS	MPA	Digested proteins	5	-	ESI-MS	[100]
CdS	ATP, MUA	Peptides and proteins	15–30	0.01–63 nM	MALDI-MS	[101]
CdSe	MUA	Peptides and proteins	<10	-	LDI-MS	[102]
Cd ²⁺ -doped CNTs- CdS NPs	-	Cytochrome c and lysozyme	-	1–7 nM	AP-MALDI-MS and MALDI-MS	[103]
ZnSe	MPA	Leu-enk, Met-enk, HW6, substance P and Angio-II, and proteins (cytochrome c, myoglobin and lysozyme)	<5	-	MALDI-MS	[104]
ZnSe	MPA	Insulin, ubiquitin, cytochrome c, myoglobin and lysozyme	<10	-	MALDI-MS	[105]
Mn ²⁺ -ZnS	Cysteine	Peptides and proteins	5.1	~1.0 pM	MALDI MS	[91]
HgTe	MPA	Angio- I, Insulin, cytochrome c, BSA, IgG and <i>E. coli</i>	20	0.2–450 nM	SALDI- and MALDI-MS	[90]
HgTe	MPA	α_1 -antitrypsin–trypsin and IgG–protein G complexes,	-	0.5–3.0 μ M	MALDI-MS	[106]
CdS:Mn/ZnS	DDTC	Tryptic digests of cytochrome c, lysozyme and BSA	6 \pm 2	-	MALDI-MS	[107]
BaTiO ₃	-	Tryptic digests of α - and β - casein and milk proteins	30	-	MALDI-MS	[108]
SnO ₂ and TiO ₂	PMMA	Myoglobin	2–8	1 nM	SALDI-MS	[109]
Au, TiO ₂ , Se, CdTe QDs, Fe ₃ O ₄ , and Pt	-	Glutathione, Angio-I, insulin, cytochrome c and chymotrypsin	-	140–4400 fM	SALDI-MS	[110]
Mg(OH) ₂	Oleic acid	Gramicidin D, valinomycin, <i>E. coli</i>	<35	-	MALDI-MS	[111]

Table 2. Cont.

Name of semiconductor NPs	Capping ligand	Analytes	Size (nm)	Detection limit	Technique	Reference
ZnO	-	<i>E. coli</i>	-	-	MALDI-MS	[112]
ZnO	-	<i>Staphylococcus aureus</i>	-	-	MALDI-MS	[113]
CdS	MPA	Extracellular polysaccharides in <i>E. coli</i>	<5	-	MALDI-MS	[114]
TiO ₂	-	<i>Staphylococcus aureus</i>	-	-	MALDI-MS	[115]
TiO ₂	bacteria	<i>Staphylococcus aureus subsp. aureus</i> and <i>Pseudomonas aeruginosa</i>	-	-	MALDI-MS	[116]
ZrO ₂ and ZrO ₂ -SiO ₂	-	Leu-enk, Met-enk, HW6, and milk proteins	20–30	75–105 fM	AP-MALDI-MS	[117]
TiO ₂ -dopamine and TiO ₂ -CdS	-	Gramicidin D, myoglobin, cytochrome c, α - and β -caseins	5–20	1 nM	MALDI-MS	[118]
BaTiO ₃	HOA	PLs and Hydrophobic proteins in <i>E. coli</i>	30–40	0.20–0.40 μ M	MALDI-MS	[119]

5. Conclusions and Future Perspectives

The possibility to control and tune the unique optical and electronic properties of semiconductor NMs through their dimensions paves the way to the application of nanomaterials-based fluorescence spectrometric and MALDI-MS as versatile analytical tools. The need for ultrasensitive bioassays and the trend towards miniaturized assays have made the semiconductor nanomaterials-based fluorescence spectroscopy and MALDI-MS approaches to be the most popular field in proteomics research. A wide variety of semiconductor nanomaterials have been introduced into fluorescence spectroscopy and MALDI-MS for sensitive identification of proteins from various biological samples. Semiconductor nanomaterials can be used as optical probes and affinity/concentrating probes to enhance/decrease fluorescent signals in fluorescence spectroscopy and to enrich/enhance trace level proteins signals in MALDI-MS. The functionalized semiconductors QDs have showed high ability to quench/enhance or trap/concentrate the target analytes in fluorescence spectroscopy and MALDI-MS. These approaches are based on the dipole-dipole interaction in fluorescence and covalent or hydrophobic or electrostatic interactions in MALDI-MS. On the basis of the current state of art in nanomaterials-based bioanalytical tools, semiconductor nanomaterials-based fluorescence spectroscopy and MALDI-MS approaches are efficient tools for rapid and sensitive identification of biomolecules in modern proteomic research.

For QDs-based fluorescence approaches based on the FRET principle, tuning electronic property of QDs by controllable modification and organic framework on QDs surfaces, and development of techniques to integrate QDs into practical devices having high sensitivity, selectivity with acceptable reproducibility, reliability, non-toxic and low cost remains a big challenge. As for QD-based fluorescent probes, although QDs have distinct advantages over organic dyes such as high fluorescent ability, biocompatibility, facile functionalization and extremely bright (40%–80% room temperature quantum efficiency) emission tunable to any desired wavelength in the spectral range of 500–800 nm. The use of organic framework on QDs surfaces not only permits for efficient FRET but also allows for a purposeful design of a wide variety of organic (dyes, conjugated polymers) and strong interactions with target analytes, which enhances the optical and conducting properties of QDs with robustness and flexibility. Therefore, surface chemistry should be designed taking into consideration the chemical nature of the semiconductor QDs and at the same time affording efficient ligand coupling and providing optimal ligand presentation. Furthermore, there is a great demand for effective surface coupling chemistry for controlled coupling with bioactive species to enable specific targeting in cellular and *in vivo* imaging of biomedical samples. The organic framework on QDs surfaces is likely to continue, which should be highly beneficial to the overall development and mechanistic understanding of semiconductor QDs as fluorescent probes for biomolecule assays as more competitive alternatives to conventional organic dyes.

The supramolecular chemistry of QDs coupled MALDI-MS provides an excellent reproducibility, high mass resolution, allows quantitative determination of concentrations of a wide variety of biomolecules (peptides and large proteins > 1.0 kDa). Semiconductor QDs-based MALDI approaches proved as a powerful bioanalytical tools, providing the advantages of multifunctional roles (as heat absorbers and as affinity probes) and ease of sample preparation for proteomics. To this end, development of suitable chemical routes and organic framework approaches for precise control over

size, size distribution, morphology and active reacting groups of QDs is urgently needed, as this is closely correlated to the performance of the QDs-based MALDI-MS approaches for biomolecules assays and for the safety issues as well. Although these QDs-based MALDI-MS proved a powerful bioanalytical tool for proteomics studies, much more work remains to be done for the applications of QDs in MALDI-MS and MALDI imaging mass spectrometry to enable specific targeting in cellular and *in vivo* imaging and related biomedical applications.

Acknowledgements

We thank the National Sun Yat-Sen University and Kaohsiung Medical University Joint Research Project (NSYSU-KMU JOINT RESEARCH PROJECT, #NSYSU-KMU2013-I005) for financial support for this publication.

Conflicts of Interest

The authors declare no conflict of interest.

References

1. Alivisatos, A.P.; Gu, W.; Larabell, C. Quantum dots as cellular probes. *Annu. Rev. Biomed. Eng.* **2005**, *7*, 55–76.
2. Zhang, L.; Gu, F.X.; Chan, J.M.; Wang, A.Z.; Langer, R.S.; Farokhzad, O.C. Nanoparticles in medicine: Therapeutic applications and developments. *Clin. Pharmacol. Ther.* **2007**, *83*, 761–769.
3. Liu, T.; Liu, B.; Zhang, H.; Wang, Y. The fluorescence bioassay platforms on quantum dots nanoparticles. *J. Fluoresc.* **2005**, *15*, 729–733.
4. Willard, D.M. Nanoparticles in bioanalytics. *Anal. Bioanal. Chem.* **2003**, *376*, 284–286.
5. Mirzaei, J.; Reznikov, M.; Hegmann, T. Quantum dots as liquid crystal dopants. *J. Mater. Chem.* **2012**, *22*, 22350–22365.
6. Dorfs, D.; Krahne, R.; Falqui, A.; Manna, L.; Giannini, C.; Zanchet, D. *Synthesis and Characterization of Quantum Dots*; Andrews, D., Scholes, G., Wiederrecht, G., Eds.; Comprehensive Nanoscience and Technology Elsevier, Academic Press: San Diego, CA, USA, 2011; pp. 219–270.
7. Rogach, A.L. Fluorescence energy transfer in hybrid structures of semiconductor nanocrystals. *Nano Today* **2011**, *6*, 355–365.
8. Wise, F.W. Lead salt quantum dots: The limit of strong quantum confinement. *Acc. Chem. Res.* **2000**, *33*, 773–780.
9. Somers, R.C.; Bawendi, M.G.; Nocera, D.G. CdSe nanocrystal based chem-/bio-sensors. *Chem. Soc. Rev.* **2007**, *36*, 579–591.
10. Kailasa, S.K.; Wu, H.F.; Mehta, V. Prospects of engineering quantum dots applications in ultrasensitive assays. In *Quantum Dots: Applications, Synthesis and Characterization*; Orion, C., Ed.; Nova Science Publishers: Hauppauge, NY, USA, 2012; Chapter 5, pp. 69–108.
11. Henglein, A. Small-particle research—Physicochemical properties of extremely small colloidal metal and semiconductor particles. *Chem. Rev.* **1989**, *89*, 1861–1873.

12. Wang, Y.; Herron, N. Nanometer-sized semiconductor clusters-materials synthesis, quantum size effects, and photophysical properties. *J. Phys. Chem.* **1991**, *95*, 525–532.
13. *Miniaturization*; Gilbert, H.D., Ed.; Reinhold: New York, NY, USA, 1961; pp. 282–296.
14. Talapin, D.V.; Rogach, A.L.; Kornowski, A.; Haase, M.; Weller, H. Highly luminescent monodisperse CdSe and CdSe/ZnS nanocrystals synthesized in a hexadecylamine– trioctylphosphine oxide–trioctylphosphine mixture. *Nano Lett.* **2001**, *1*, 207–211.
15. Franzl, T.; Muller, J.; Klar, T.A.; Rogach, A.L.; Feldmann, J.; Talapin, D.V.; Weller, H. CdSe:Te nanocrystals: Band-edge vs. Te-Related emission. *J. Phys. Chem. C* **2007**, *111*, 2974–2979.
16. Brus, L.E. Electron–electron and electron-hole interactions in small semiconductor crystallites: The size dependence of the lowest excited electronic state. *J. Chem. Phys.* **1984**, *80*, 4403–4409.
17. Bawendi, M.G.; Steigerwald, M.L.; Brus, L.E. The quantum mechanics of larger semiconductor clusters (“Quantum Dots”). *Annu. Rev. Phys. Chem.* **1990**, *41*, 477–496.
18. Brus, L.E. A simple model for the ionization potential, electron affinity, and aqueous redox potentials of small semiconductor crystallites. *J. Chem. Phys.* **1983**, *79*, 5566–5571.
19. Gaponenko, S.V. *Optical Properties of Semiconductor Nanocrystals*; Cambridge University Press: Cambridge, UK, 1999.
20. Poole, C.P.; Owens, F.J. *Introduction to Nanotechnology*; John Wiley & Sons: Hoboken, NJ, USA, 2003.
21. Kittel, C. *Introduction to Solid State Physics*; John Wiley & Sons: Hoboken, NJ, USA, 2003.
22. Harrison, P. *Quantum Well, Wires, and Dots*; John Wiley & Sons: Hoboken, NJ, USA, 2003.
23. Leatherdale, C.A.; Woo, W.K.; Mikulec, F.V.; Bawendi, M.G. On the absorption cross section of CdSe nanocrystal quantum dots. *J. Phys. Chem. B* **2002**, *106*, 7619–7622.
24. Smith, A.M.; Nie, S. Semiconductor nanocrystals: Structure, properties, and band gap engineering. *Acc. Chem. Res.* **2010**, *43*, 190–200.
25. Pokrant, S.; Whaley, K.B. Tight-binding studies of surface effects on electronic structure of CdSe nanocrystals: The role of organic ligands, surface reconstruction, and inorganic capping shells. *Eur. Phys. J. D* **1999**, *6*, 255–267.
26. Underwood, D.F.; Kippeny, T.; Rosenthal, S.J. Ultrafast carrier dynamics in CdSe nanocrystals determined by femtosecond fluorescence upconversion spectroscopy. *J. Phys. Chem. B* **2001**, *105*, 436–443.
27. Murphy, C.J. Peer reviewed: Optical sensing with quantum dots. *Anal. Chem.* **2002**, *74*, 520A–526A.
28. Clapp, A.R.; Medintz, I.L.; Mattoussi, H. Förster resonance energy transfer investigations using quantum-dot fluorophores. *Chem. Phys. Chem.* **2006**, *7*, 47–57.
29. Tian, Z.; Wu, W.; Li, A.D.Q. Photoswitchable nanoprobe for biological imaging applications. In *Trace Analysis with Nanomaterials*; Pierce, D.T., Zhao, J.X., Eds.; Springer: Berlin, Germany, 2007; Chapter 1, pp. 3–8.
30. Banerjee, S.; Kar, S.; Perez, J.M.; Santra, S. Quantum dot-based OFF/ON probe for detection of glutathione. *J. Phys. Chem. C* **2009**, *113*, 9659–9666.
31. Santra, S.; Yang, H.; Holloway, P.H.; Stanley, J.T.; Mericle, R.A. Synthesis of water-dispersible fluorescent, radio-opaque, and paramagnetic CdS:Mn/ZnS quantum dots: A multifunctional probe for bioimaging. *J. Am. Chem. Soc.* **2005**, *127*, 1656–1657.

32. Liu, J.; Bao, C.; Zhong, X.; Zhao, C.; Zhu, L. Highly selective detection of glutathione using a quantum-dot-based OFF-ON fluorescent probe. *Chem. Commun.* **2010**, *46*, 2971–2973.
33. Li, H.; Shih, W.H.; Shih, W.Y. Synthesis and characterization of aqueous carboxyl-capped CdS quantum dots for bioapplications. *Ind. Eng. Chem. Res.* **2007**, *46*, 2013–2019.
34. Baruah, S.; Ortinero, C.; Shipin, O.V.; Dutta, J. Manganese doped zinc sulfide quantum dots for detection of *Escherichia coli*. *J. Fluoresc.* **2012**, *22*, 403–408.
35. Chang, S.Q.; Kang, B.; Dai, Y.D.; Zhang, H.X.; Chen, D. One-step fabrication of biocompatible chitosan-coated ZnS and ZnS:Mn²⁺ quantum dots via a γ -radiation route. *Nanoscale Res. Lett.* **2011**, *6*, 591–597.
36. Shi, W.; Ma, X. The detection application of CdS quantum dots in labeling DNA molecules. *Biomed. Mater.* **2006**, *1*, 81–84.
37. Shi, W.; Ma, X. Labeling patterned DNA molecules using CdS fluorescence nanoparticles. *J. Nanosci. Nanotechnol.* **2009**, *9*, 965–968.
38. Zhang, B.; Zhang, Y.; Mallapragada, S.K.; Clapp, A.R. Sensing polymer/DNA polyplex dissociation using quantum dot fluorophores. *ACS Nano* **2011**, *25*, 129–138.
39. Ho, Y.P.; Kung, M.C.; Yang, S.; Wang, T.H. Multiplexed hybridization detection with multicolor colocalization of quantum dot nanoprobe. *Nano Lett.* **2005**, *5*, 1693–1697.
40. Akerman, M.E.; Chan, W.C.; Laakkonen, P.; Bhatia, S.N.; Ruoslahti, E. Nanocrystal targeting *in vivo*. *Proc. Natl. Acad. Sci. USA* **2002**, *99*, 12617–12621.
41. Larson, D.R.; Zipfel, W.R.; Williams, R.M.; Clark, S.W.; Bruchez, M.P.; Wise, F.W.; Webb, W.W. Water-soluble quantum dots for multiphoton fluorescence imaging *in vivo*. *Science* **2003**, *300*, 1434–1436.
42. Gao, X.; Cui, Y.; Levenson, R.M.; Chung, L.W.; Nie, S. *In vivo* cancer targeting and imaging with semiconductor quantum dots. *Nat. Biotechnol.* **2004**, *22*, 969–976.
43. Wu, Q.; Li, Y.; Wang, M.; Wu, Z.G.; Huang, B.H. Rapid identification of *Staphylococcus aureus* directly from positive blood culture media using quantum dots as fluorescence probes. *APMIS* **2013**, *121*, 348–352.
44. Osaki, F.; Kanamori, T.; Sando, S.; Sera, T.; Aoyagi, Y. A quantum dot conjugated sugar ball and its cellular uptake. On the size effects of endocytosis in the subviral region. *J. Am. Chem. Soc.* **2004**, *126*, 6520–6521.
45. Kaul, Z.; Yaguchi, T.; Kaul, S.C.; Hirano, T.; Wadhwa, R.; Taira, K. Mortalin imaging in normal and cancer cells with quantum dot immuno-conjugates. *Cell Res.* **2003**, *13*, 503–507.
46. Frasco, M.F.; Chaniotakis, N. Semiconductor quantum dots in chemical sensors and biosensors. *Sensors* **2009**, *9*, 7266–7286.
47. Han, C.; Li, H. Host-molecule-coated quantum dots as fluorescent sensors. *Anal. Bioanal. Chem.* **2010**, *397*, 1437–1444.
48. Mattoussi, H.; Mauro, J.M.; Goldman, E.R.; Anderson, G.P.; Sundar, V.C.; Mikulec, F.V.; Bawendi, M.G. Self-assembly of CdSe-ZnS quantum dot bioconjugates using an engineered recombinant protein. *J. Am. Chem. Soc.* **2000**, *122*, 12142–12150.
49. Goldman, E.R.; Mattoussi, H.; Anderson, G.P.; Medintz, I.L.; Mauro, J.M. Fluoroimmunoassays using antibody-conjugated quantum dots. *Methods Mol. Biol.* **2005**, *303*, 19–34.

50. Goldman, E.R.; Clapp, A.R.; Anderson, G.P.; Uyeda, H.T.; Mauro, J.M.; Medintz, I.L.; Mattoussi, H. Multiplexed toxin analysis using four colors of quantum dot fluororeagents. *Anal. Chem.* **2004**, *76*, 684–688.
51. Lao, U.L.; Mulchandani, A.; Chen, W. Simple conjugation and purification of quantum dot-antibody complexes using a thermally responsive elastin-protein L scaffold as immunofluorescent agents. *J. Am. Chem. Soc.* **2006**, *128*, 14756–14757.
52. Huang, S.; Xiao, Q.; He, Z.K.; Liu, Y.; Tinnefeld, P.; Su, X.R.; Peng, X.N. A high sensitive and specific QDs FRET bioprobe for MNase. *Chem. Commun.* **2008**, 5990–5992.
53. Medintz, I.L.; Clapp, A.R.; Brunel, F.M.; Tiefenbrunn, T.; Uyeda, H.T.; Chang, E.L.; Deschamps, J.R.; Dawson, P.E.; Mattoussi, H. Proteolytic activity monitored by fluorescence resonance energy transfer through quantum-dot-peptide conjugates. *Nat. Mater.* **2006**, *5*, 581–589.
54. Prasuhn, D.E.; Feltz, A.; Blanco-Canosa, J.B.; Susumu, K.; Stewart, M.H.; Mei, B.C.; Yakovlev, A.V.; Loukov, C.; Mallet, J.M.; Oheim, M.; *et al.* Quantum dot peptide biosensors for monitoring caspase 3 proteolysis and calcium ions. *ACS Nano* **2010**, *4*, 5487–5497.
55. Boeneman, K.; Mei, B.C.; Dennis, A.M.; Bao, G.; Deschamps, J.R.; Mattoussi, H.; Medintz, I.L. Sensing caspase 3 activity with quantum dot-fluorescent protein assemblies. *J. Am. Chem. Soc.* **2009**, *131*, 3828–3829.
56. Hildebrandt, N.; Geissler, D. Semiconductor quantum dots as FRET acceptors for multiplexed diagnostics and molecular ruler application. *Adv. Exp. Med. Biol.* **2012**, *733*, 75–86.
57. Algar, W.R.; Wegner, D.; Huston, A.L.; Blanco-Canosa, J.B.; Stewart, M.H.; Armstrong, A.; Dawson, P.E.; Hildebrandt, N.; Medintz, I.L. Quantum dots as simultaneous acceptors and donors in time-gated Förster resonance energy transfer relays: Characterization and biosensing. *J. Am. Chem. Soc.* **2012**, *134*, 1876–1891.
58. Morgner, F.; Geissler, D.; Stufler, S.; Butlin, N.G.; Löhmannsröben, H.G.; Hildebrandt, N. A quantum-dot-based molecular ruler for multiplexed optical analysis. *Angew. Chem. Int. Ed. Engl.* **2010**, *49*, 7570–7574.
59. Morgner, F.; Stufler, S.; Geissler, D.; Medintz, I.L.; Algar, W.R.; Susumu, K.; Stewart, M.H.; Blanco-Canosa, J.B.; Dawson, P.E.; Hildebrandt, N. Terbium to quantum dot FRET bioconjugates for clinical diagnostics: Influence of human plasma on optical and assembly properties. *Sensors* **2011**, *11*, 9667–9684.
60. Geissler, D.; Charbonnière, L.J.; Ziessel, R.F.; Butlin, N.G.; Löhmannsröben, H.G.; Hildebrandt, N. Quantum dot biosensors for ultrasensitive multiplexed diagnostics. *Angew. Chem. Int. Ed. Engl.* **2010**, *49*, 1396–1401.
61. Choi, J.H.; Chen, K.H.; Strano, M.S. Aptamer-capped nanocrystal quantum dots: A new method for label-free protein detection. *J. Am. Chem. Soc.* **2006**, *128*, 15584–15585.
62. Levy, M.; Cater, S.F.; Ellington, A.D. Quantum-dot aptamer beacons for the detection of proteins. *ChemBioChem* **2005**, *6*, 2163–2166.
63. Zhang, Y.; So, M.-K.; Loening, A.M.; Yao, H.; Gambhir, S.S.; Rao, J. HaloTag protein-mediated site-specific conjugation of bioluminescent proteins to quantum dots. *Angew. Chem. Int. Ed.* **2006**, *45*, 4936–4940.

64. Xia, Z.; Xing, Y.; So, M.-K.; Koh, A.L.; Sinclair, R.; Rao, J. Multiplex detection of protease activity with quantum dot nanosensors prepared by intein-mediated specific bioconjugation. *Anal. Chem.* **2008**, *80*, 8649–8655.
65. Ma, Q.; Wang, X.; Li, Y.; Shi, Y.; Su, X. Multicolor quantum dot-encoded microspheres for the detection of biomolecules. *Talanta* **2007**, *72*, 1446–1452.
66. Song, E.Q.; Zhang, Z.L.; Luo, Q.Y.; Lu, W.; Shi, Y.B.; Pang, D.W. Tumor cell targeting using folate-conjugated fluorescent quantum dots and receptor-mediated endocytosis. *Clin. Chem.* **2009**, *55*, 955–963.
67. Liu, W.; Howarth, M.; Greytak, A.B.; Zheng, Y.; Nocera, D.G.; Ting, A.Y.; Bawendi, M.G. Compact biocompatible quantum dots functionalized for cellular imaging. *J. Am. Chem. Soc.* **2008**, *130*, 1274–1284.
68. Kikkeri, R.; Lepenies, B.; Adibekian, A.; Laurino, P.; Seeberger, P.H. *In vitro* imaging and *in vivo* liver targeting with carbohydrate capped quantum dots. *J. Am. Chem. Soc.* **2009**, *131*, 2110–2112.
69. Zhang, C.Y.; Yeh, C.H.; Kuroki, M.; Wang, T.H. Single-quantum-dot-based DNA nanosensor. *Nat. Mater.* **2005**, *4*, 826–831.
70. Peng, H.; Zhang, L.; Kjallman, T.H.M.; Soeller, C.; Sejdic, J.T. DNA hybridization detection with blue luminescent quantum dots and dye-labeled single-stranded DNA. *J. Am. Chem. Soc.* **2007**, *129*, 3048–3049.
71. Wu, C.S.; Cupps, J.M.; Fan, X.D. Compact quantum dot probes for rapid and sensitive DNA detection using highly efficient fluorescence resonant energy transfer. *Nanotechnology* **2009**, *20*, doi:10.1088/0957-4484/20/30/305502.
72. Kim, Y.S.; Kim, B.C.; Lee, J.H.; Kim, J.B.; Gu, M.B. Specific detection of DNA using quantum dots and magnetic beads for large volume samples. *Biotechnol. Bioprocess Eng.* **2006**, *11*, 449–454.
73. Xue, X.; Pan, J.; Xie, H.; Wang, J.; Zhang, S. Fluorescence detection of total count of *Escherichia coli* and *Staphylococcus aureus* on water-soluble CdSe quantum dots coupled with bacteria. *Talanta* **2009**, *77*, 1808–1813.
74. Wang, Q.; Ye, F.; Fang, T.; Niu, W.; Liu, P.; Min, X.; Li, X. Bovine serum albumin-directed synthesis of biocompatible CdSe quantum dots and bacteria labeling. *J. Colloid Interface Sci.* **2011**, *355*, 9–14.
75. Jackeray, R.; Abid, C.K.V.Z.; Singh, G.; Jain, S.; Chattopadhyaya, S.; Sapra, S.; Shrivastav, T.G.; Singh, H. Selective capturing and detection of *Salmonella typhi* on polycarbonate membrane using bioconjugated quantum dots. *Talanta* **2011**, *84*, 952–962.
76. Zhang, L.Y.; Zheng, H.Z.; Long, Y.J.; Huang, C.Z.; Hao, J.Y.; Zhou, D.B. CdTe quantum dots as a highly selective probe for prion protein detection: Colorimetric qualitative, semi-quantitative and quantitative detection. *Talanta* **2011**, *83*, 1716–1720.
77. Ma, Y.; Bai, H.; Yang, C.; Yang, X. A sensitive method for the detection of proteins by high-efficiency fluorescence quenching. *Analyst* **2005**, *130*, 283–285.
78. Ju, P.; Fan, H.; Liu, T.; Cui, L.; Ai, S. Probing the interaction of flower-like CdSe nanostructure particles targeted to bovine serum albumin using spectroscopic techniques. *J. Lumin.* **2011**, *131*, 1724–1730.

79. Depalo, N.; Mallardi, A.; Comparelli, R.; Striccoli, M.; Agostiano, A.; Curri, M.L. Bovine serum albumin-directed synthesis of biocompatible CdSe quantum dots and bacteria labeling. *J. Colloid Interface Sci.* **2008**, *325*, 558–566.
80. Ge, S.; Lu, J.; Yan, M.; Yu, F.; Yu, J.; Sun, X. Fluorescence resonance energy transfer sensor between quantum dot donors and neutral red acceptors and its detection of BSA in micelles. *Dye. Pigment.* **2011**, *91*, 304–308.
81. Peng, J.; Liu, S.; Yan, S.; Fan, X.; He, Y. A study on the interaction between CdTe quantum dots and chymotrypsin using optical spectroscopy. *Colloids Surf. A* **2010**, *359*, 13–17.
82. He, Y.; Yin, P.; Gong, H.; Peng, J.; Liu, S.; Fan, X.; Yan, S. Characterization of the interaction between mercaptoethylamine capped CdTe quantum dots with human serum albumin and its analytical application. *Sens. Actuators B* **2011**, *157*, 8–13.
83. Lai, L.; Lin, C.; Xu, Z.Q.; Han, X.L.; Tian, F.F.; Mei, P.; Li, D.W.; Ge, Y.S.; Jiang, F.L.; Zhang, Y.Z.; *et al.* Spectroscopic studies on the interactions between CdTe quantum dots coated with different ligands and human serum albumin. *Spectrochim. Acta A* **2012**, *97*, 366–376.
84. Xiao, J.; Bai, Y.; Wang, Y.; Chen, J.; Wei, X. Systematic investigation of the influence of CdTe QDs size on the toxic interaction with human serum albumin by fluorescence quenching method. *Spectrochim. Acta A* **2010**, *76*, 93–97.
85. Xiao, Q.; Huang, S.; Su, W.; Li, P.; Ma, J.; Luo, F.; Chen, J.; Liu, Y. Systematically investigations of conformation and thermodynamics of HSA adsorbed to different sizes of CdTe quantum dots. *Colloids Surf. B* **2013**, *102*, 76–82.
86. Wang, Q.; Zhang, X.; Zhou, X.; Fang, T.; Liu, P.; Liu, P.; Min, X.; Li, X. Interaction of different thiol-capped CdTe quantum dots with bovine serum albumin. *J. Lumin.* **2012**, *132*, 1695–1700.
87. Zhu, C.Q.; Zhao, D.H.; Chen, J.L.; Li, Y.X.; Wang, L.Y.; Wang, L.; Zhou, Y.Y.; Zhuo, S.J.; Wu, Y.Q. Application of L-cysteine-capped nano-ZnS as a fluorescence probe for the determination of proteins. *Anal. Bioanal. Chem.* **2004**, *378*, 811–815.
88. Li, L.; Zhang, F.; Ding, Y.; Wang, Y.; Zhang, L. Synthesis of functionalized ZnSe nanoparticles and their applications in the determination of bovine serum albumin. *J. Fluoresc.* **2009**, *19*, 437–441.
89. Wang, X.; Wu, J.; Li, F.; Li, H. Synthesis of water-soluble CdSe quantum dots by ligand exchange with p-sulfonatocalix(n)arene (n = 4, 6) as fluorescent probes for amino acids. *Nanotechnology* **2008**, *19*, 205501–205508.
90. Chiang, C.K.; Yang, Z.; Lin, Y.W.; Chen, W.T.; Lin, H.J.; Chang, H.T. Detection of proteins and protein-ligand complexes using HgTe nanostructure matrixes in surface-assisted laser desorption/ionization mass spectrometry. *Anal. Chem.* **2010**, *82*, 4543–4550.
91. Liu, C.W.; Chien, M.W.; Chen, G.F.; Chen, S.Y.; Yu, C.S.; Liao, M.Y.; Lai, C.C.C. Quantum dots enhance peptide detection by matrix-assisted laser desorption/ionization mass spectrometry. *Anal. Chem.* **2011**, *83*, 6593–6600.
92. Tanaka, K.; Waki, H.; Ido, Y.; Akita, S.; Yoshida, Y.; Yoshida, T. Protein and polymer analyses up to m/z 100 000 by laser ionization time-of-flight mass spectrometry. *Rapid Commun. Mass Spectrom.* **1988**, *2*, 151–153.
93. Zhu, Z.J.; Rotello, V.M.; Vachet, R.W. Engineered nanoparticle surfaces for improved mass spectrometric analyses. *Analyst* **2009**, *134*, 2183–2188.

94. Chiang, C.K.; Chen, W.T.; Chang, H.T. Nanoparticle-based mass spectrometry for the analysis of biomolecules. *Chem. Soc. Rev.* **2011**, *40*, 1269–1281.
95. Wu, H.F.; Gopal, J.; Abdelhamid, H.N.; Hasan, N. Quantum dot applications endowing novelty to analytical proteomics. *Proteomics* **2012**, *19–20*, 2949–2961.
96. Kailasa, S.K.; Kiran, K.; Wu, H.F. Comparison of ZnS semiconductor nanoparticles capped with various functional groups as the matrix and affinity probes for rapid analysis of cyclodextrins and proteins in surface-assisted laser desorption/ionization time-of-flight mass spectrometry. *Anal. Chem.* **2008**, *80*, 9681–9688.
97. Wu, H.F.; Kailasa, S.K.; Shastri, L. Electrostatically self-assembled azides on zinc sulfide nanoparticles as multifunctional nanoprobe for peptide and protein analysis in MALDI-TOF MS. *Talanta* **2010**, *82*, 540–547.
98. Kailasa, S.K.; Wu, H.F. Interference free detection for small molecules: Probing the Mn²⁺-doped effect and cysteine capped effect on the ZnS nanoparticles for coccidiostats and peptide analysis in SALDI-TOF MS. *Analyst* **2010**, *135*, 1115–1123.
99. Ke, Y.; Kailasa, S.K.; Wu, H.F.; Chen, Z.Y. High resolution detection of high mass proteins up to 80,000 Da via multifunctional CdS quantum dots in laser desorption/ionization mass spectrometry. *Talanta* **2010**, *83*, 178–184.
100. Shrivastava, K.; Kailasa, S.K.; Wu, H.F. Quantum dots—Electrospray ionization mass spectrometry: 3-Mercaptopropionic acid capped CdS quantum dots as accelerating and enrichment probes for microwave tryptic digestion of proteins. *Rapid Commun. Mass Spectrom.* **2009**, *23*, 3603–3607.
101. Kailasa, S.K.; Wu, H.F. Semiconductor cadmium sulphide nanoparticles as matrices for peptides and as co-matrices for the analysis of large proteins in matrix-assisted laser desorption/ionization reflectron and linear time-of-flight mass spectrometry. *Rapid Commun. Mass Spectrom.* **2011**, *25*, 271–280.
102. Shrivastava, K.; Kailasa, S.K.; Wu, H.F. Quantum dots laser desorption/ionization MS: Multifunctional CdSe quantum dots as the matrix, concentrating probes and acceleration for microwave enzymatic digestion for peptide analysis and high resolution detection of proteins in a linear MALDI-TOF MS. *Proteomics* **2009**, *9*, 2656–2667.
103. Shrivastava, K.; Wu, H.F. Multifunctional nanoparticles composite for MALDI-MS: Cd²⁺-doped carbon nanotubes with CdS nanoparticles as the matrix, preconcentrating and accelerating probes of microwave enzymatic digestion of peptides and proteins for direct MALDI-MS analysis. *J. Mass Spectrom.* **2010**, *45*, 1452–1460.
104. Wu, H.F.; Chung, F.T. 3-Mercaptopropionic acid modified ZnSe quantum dots as the matrix for direct surface-assisted laser desorption/ionization mass spectrometric analysis of peptides/proteins from sodium salt solution. *Rapid Commun. Mass Spectrom.* **2011**, *25*, 1779–1786.
105. Shastri, L.; Kailasa, S.K.; Wu, H.F. Cysteine-capped ZnSe quantum dots as affinity and accelerating probes for microwave enzymatic digestion of proteins via direct matrix-assisted laser desorption/ionization time-of-flight mass spectrometric analysis. *Rapid Commun. Mass Spectrom.* **2009**, *23*, 2247–2252.
106. Chen, W.T.; Chiang, C.K.; Lee, C.H.; Chang, H.T. Using surface-assisted laser desorption/ionization mass spectrometry to detect proteins and protein–protein complexes. *Anal. Chem.* **2012**, *84*, 1924–1930.

107. Kailasa, S.K.; Wu, H.F. Functionalized quantum dots modified with dopamine dithiocarbamate as the matrix for quantification of efavirenz in human plasma and as affinity probes for rapid identification of microwave tryptic digested proteins in MALDI-TOF-MS. *J. Proteomics* **2012**, *75*, 2924–2933.
108. Kailasa, S.K.; Wu, H.F. Rapid enrichment of phosphopeptides by BaTiO₃ nanoparticles after microwave-assisted tryptic digest of phosphoproteins, and their identification by MALDI-MS. *Microchim. Acta* **2012**, *179*, 83–90.
109. Xiong, H.M.; Guan, X.Y.; Jin, L.H.; Shen, W.W.; Lu, H.J.; Xia, Y.Y. Surfactant-free synthesis of SnO₂@PMMA and TiO₂@PMMA core-shell nanobeads designed for peptide/protein enrichment and MALDI-TOF MS analysis. *Angew. Chem. Int. Ed.* **2008**, *47*, 4204–4207.
110. Chiang, C.K.; Chiang, N.C.; Lin, Z.H.; Lan, G.Y.; Lin, Y.W.; Chang, H.T. Nanomaterial-based surface-assisted laser desorption/ionization mass spectrometry of peptides and proteins. *J. Am. Soc. Mass Spectrom.* **2010**, *21*, 1204–1207.
111. Kailasa, S.K.; Wu, H.F. Dispersive liquid-liquid microextraction using functionalized Mg(OH)₂ NPs with oleic acid as hydrophobic affinity probes for the analysis of hydrophobic proteins in bacteria by MALDI-MS. *Analyst* **2012**, *137*, 4490–4496.
112. Gopal, J.; Wu, H.F.; Lee, C.H. Matrix assisted laser desorption ionization time of flight mass spectrometry as a rapid and reliable technique for directly evaluating bactericidal activity: Probing the critical concentration of ZnO nanoparticles as affinity probes. *Anal. Chem.* **2010**, *82*, 9617–9621.
113. Gopal, J.; Wu, H.F.; Lee, C.H.; Manikandan, M. Tracing the pathogen staphylococcus aureus on laboratory ants using physical preconcentration coupled ZnO nanoparticle assisted MALDI-TOF MS. *Analyst* **2012**, *137*, 357–364.
114. Gopal, J.; Wu, H.F.; Gedda, G. Quantifying the degradation of extracellular polysaccharides of *Escherichia coli* by CdS quantum dots. *J. Mater. Chem.* **2011**, *21*, 13445–13451.
115. Gopal, J.; Narayana, J.; Wu, H.F. TiO₂ nanoparticle assisted mass spectrometry as biosensor of *Staphylococcus aureus*, key pathogen in nosocomial infections from air, skin surface and human nasal passage. *Biosens. Bioelectron.* **2011**, *27*, 201–206.
116. Hasan, N.; Gopal, J.; Wu, H.F. Fabrication of titanium based MALDI bacterial chip for rapid, sensitive and direct analysis of pathogenic bacteria. *Biosens. Bioelectron.* **2013**, *39*, 57–63.
117. Kailasa, S.K.; Wu, H.F. Multifunctional ZrO₂ nanoparticles and ZrO₂@SiO₂ nanorods for improved MALDI-MS analysis of cyclodextrin, peptide and phosphoproteins. *Anal. Bioanal. Chem.* **2010**, *396*, 1115–1125.
118. Ke, Y.; Kailasa, S.K.; Wu, H.F.; Nawaz, M. Surface-modified TiO₂ nanoparticles as affinity probes and as matrices for the rapid analysis of phosphopeptides and proteins in MALDI-TOF-MS. *J. Sep. Sci.* **2010**, *33*, 3400–3408.
119. Kailasa, S.K.; Wu, H.F. Surface modified BaTiO₃ nanoparticles as the matrix for phospholipids and as extracting probes for LLME of hydrophobic proteins in *Escherichia coli* by MALDI-MS. *Talanta* **2013**, *114*, 283–290.